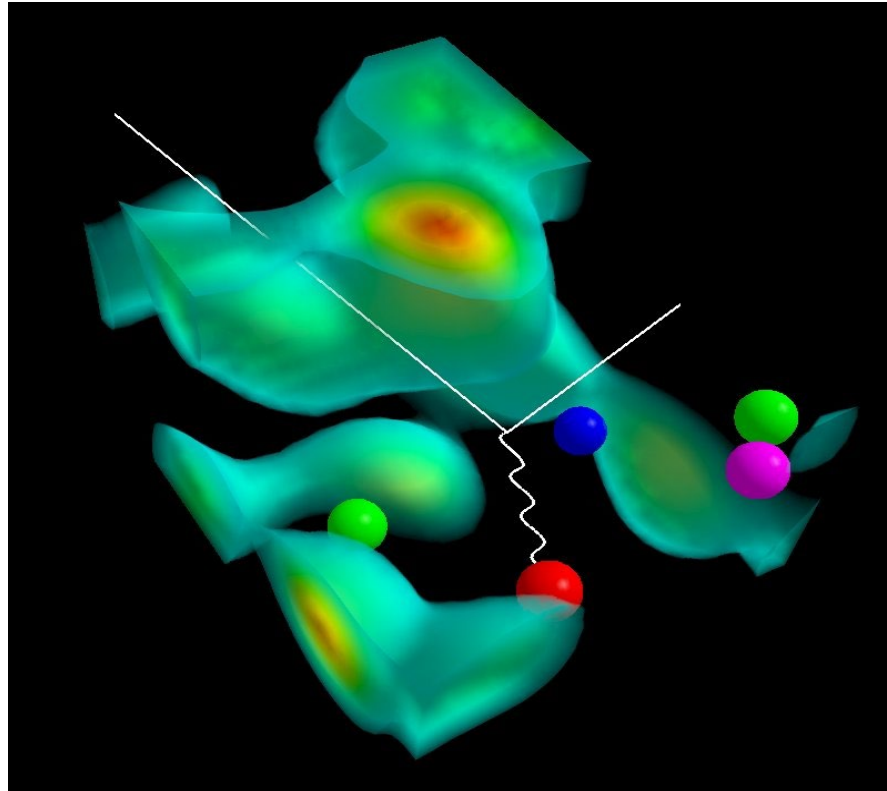


# QMC: From Quarks to Nuclei and Neutron Stars



**Anthony W. Thomas**

**ROCKSTAR**

**ECT\* Trento: October 12<sup>th</sup> 2023**

# First for something different....

RECEIVED: *May 17, 2023*REVISED: *July 21, 2023*ACCEPTED: *August 24, 2023*PUBLISHED: *September 15, 2023*

# Global QCD analysis and dark photons

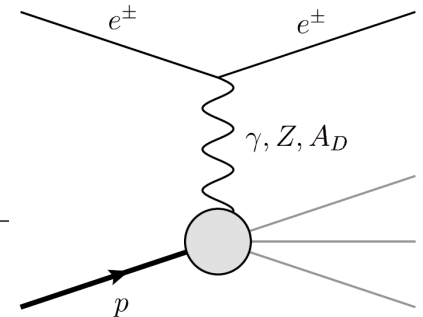
---

N. T. Hunt-Smith,<sup>a</sup> W. Melnitchouk,<sup>a,b</sup> N. Sato,<sup>b</sup> A. W. Thomas,<sup>a</sup> X. G. Wang<sup>a</sup>  
and M. J. White<sup>a</sup> on behalf of the Jefferson Lab Angular Momentum (JAM)  
collaboration

# Include Dark Photon in Analysis of World DIS data

- Use world data on DIS and Drell Yan
- Average over 200 replicas

reaction	$\chi^2_{\text{dof}}(\text{dark})$	$\chi^2_{\text{dof}}(\text{base})$	$N_{\text{dof}}$
fixed target DIS	1.01	1.05	1495
HERA NC	1.02	1.03	1104
HERA CC	1.13	1.18	81
Drell-Yan	1.18	1.16	205
Z rapidity	1.08	1.05	56
W asymmetry	1.04	1.07	97
jets	1.16	1.15	200
<b>total</b>	<b>1.03</b>	<b>1.05</b>	<b>3283</b>



- Calculate chisq for > 3,000 data points

# Next Allow for Existence: SURPRISE

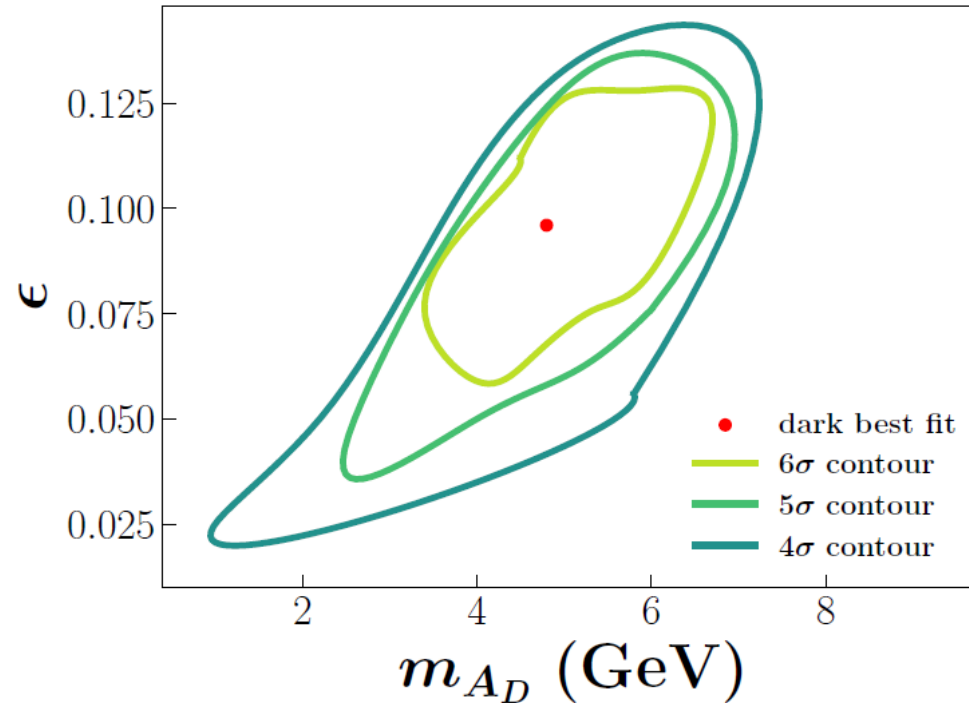


**Figure 3:** Results of an hypothesis test for the likelihood that the SM is the correct theory to describe this data, compared with the case where a dark photon is included. The hypothesis that the SM is the correct theory is excluded at  $6.5\sigma$  for the best dark photon fit at the red point.

**Solution was required to not violate the muon g-2 anomaly  
– in fact it reduces the anomaly from  $4.2\sigma$  to  $1.5\sigma$**

**Now back to the topic of this meeting**

# Outline



- I. Why the **quark**-meson coupling (QMC) model?
  - vital role of changing baryon structure in-medium
  
- II. Application of EDF derived from QMC to nuclear properties across the periodic table
  
- III. Hypernuclei: predictions involve NO new parameters : potential tests of changes in baryon structure
  
- IV. Neutron stars: role of hyperons

# I. Insights into nuclear structure

– what is the atomic nucleus?

There are two very different extremes....



# Quark Structure matters/doesn't matter

- **Nuclear femtography: the science of mapping the quark and gluon structure of *atomic nuclei* is just beginning (EIC motivation)**
- **“Considering quarks is in contrast to our **modern understanding of nuclear physics...** the basic degrees of freedom of QCD (quarks and gluons) have to be considered only at higher energies. The *energies relevant for nuclear physics are only a few MeV*”**

# What do we know?

- Since 1970s: Dispersion relations → intermediate range NN attraction is a strong Lorentz scalar
- In relativistic treatments (RHF, RBHF, QHD...) this leads to mean scalar field on a nucleon ~300 to 500 MeV!!
- *This is not small* – up to half the nucleon mass  
- death of “wrong energy scale” arguments
- Largely cancelled by large vector mean field BUT these have totally different dynamics:  $\omega^0$  just shifts energies,  $\sigma$  seriously modifies internal hadron dynamics

# Self-consistent solution for confined quarks in a hadron in nuclear matter Guichon 1988

$$[i\gamma^\mu \partial_\mu - (m_q - g_\sigma q \bar{\sigma}) - \gamma^0 g_\omega q \bar{\omega}] \psi = 0$$

Source of  $\sigma$   
changes:

$$\int_{Bag} d\vec{r} \bar{\psi}(\vec{r}) \psi(\vec{r})$$

**SELF-CONSISTENCY**

and hence mean scalar field changes...

and hence quark wave function changes....

**THIS PROVIDES A NATURAL SATURATION MECHANISM  
(VERY EFFICIENT BECAUSE QUARKS ARE LIGHT)**

**source is suppressed as mean scalar field increases  
(i.e. as density increases)**

# Quark-Meson Coupling Model (QMC): Role of the Scalar Polarizability of the Nucleon

The response of the nucleon internal structure to the scalar field is of great interest... and importance

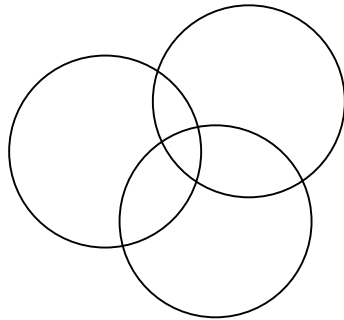
$$M^*(\mathbf{r}) = M - g_\sigma \sigma(\mathbf{r}) + \frac{d}{2} (g_\sigma \sigma(\mathbf{r}))^2$$

Non-linear dependence through the scalar polarizability  
 $d \sim 0.22 R$  in original QMC (MIT bag)

Indeed, in nuclear matter at mean-field level,  
this is the **ONLY** place the response of the  
internal structure of the nucleon enters.

# Summary : Scalar Polarizability

- Consequence of polarizability in atomic physics is many-body forces:



$$V = V_{12} + V_{23} + V_{13} + V_{123}$$

– same is true in nuclear physics

- Three-body forces (for ALL baryons: NNN, HNN, HHN...)  
generated with NO new parameters  
– critical in neutron stars

# Application to nuclear structure

# Initial Derivation of Density Dependent Effective Force

Physical origin of density dependent forces of Skyrme type within the quark meson coupling model

P.A.M. Guichon <sup>a,\*</sup>, H.H. Matevosyan <sup>b,c</sup>, N. Sandulescu <sup>a,d,e</sup>,  
A.W. Thomas <sup>b</sup>

Nuclear Physics A 772 (2006) 1–19

- **Start with classical theory of MIT-bag nucleons with structure modified in medium to give  $M_{\text{eff}}(\sigma)$ .**
- **Quantise nucleon motion (non-relativistic), expand in powers of derivatives**
- **Derive equivalent, local energy density functional:**

$$\langle H(\vec{r}) \rangle = \rho M + \frac{\tau}{2M} + \mathcal{H}_0 + \mathcal{H}_3 + \mathcal{H}_{\text{eff}} + \mathcal{H}_{\text{fin}} + \mathcal{H}_{\text{so}}$$

# Derivation of EDF (cont.)

$$\mathcal{H}_0 + \mathcal{H}_3 = \rho^2 \left[ \frac{-3G_\rho}{32} + \frac{G_\sigma}{8(1 + d\rho G_\sigma)^3} - \frac{G_\sigma}{2(1 + d\rho G_\sigma)} + \frac{3G_\omega}{8} \right] \\ + (\rho_n - \rho_p)^2 \left[ \frac{5G_\rho}{32} + \frac{G_\sigma}{8(1 + d\rho G_\sigma)^3} - \frac{G_\omega}{8} \right],$$

$$\mathcal{H}_{\text{eff}} = \left[ \left( \frac{G_\rho}{8m_\rho^2} - \frac{G_\sigma}{2m_\sigma^2} + \frac{G_\omega}{2m_\omega^2} + \frac{G_\sigma}{4M_N^2} \right) \rho_n + \left( \frac{G_\rho}{4m_\rho^2} + \frac{G_\sigma}{2M_N^2} \right) \rho_p \right] \tau_n \\ + p \leftrightarrow n,$$

$$\mathcal{H}_{\text{fin}} = \left[ \left( \frac{3G_\rho}{32m_\rho^2} - \frac{3G_\sigma}{8m_\sigma^2} + \frac{3G_\omega}{8m_\omega^2} - \frac{G_\sigma}{8M_N^2} \right) \rho_n \right. \\ \left. + \left( \frac{-3G_\rho}{16m_\rho^2} - \frac{G_\sigma}{2m_\sigma^2} + \frac{G_\omega}{2m_\omega^2} - \frac{G_\sigma}{4M_N^2} \right) \rho_p \right] \nabla^2(\rho_n) + p \leftrightarrow n,$$

$$\mathcal{H}_{\text{so}} = \nabla \cdot J_n \left[ \left( \frac{-3G_\sigma}{8M_N^2} - \frac{3G_\omega(-1 + 2\mu_s)}{8M_N^2} - \frac{3G_\rho(-1 + 2\mu_v)}{32M_N^2} \right) \rho_n \right. \\ \left. + \left( \frac{-G_\sigma}{4M_N^2} + \frac{G_\omega(1 - 2\mu_s)}{4M_N^2} \right) \rho_p \right] + p \leftrightarrow n.$$

**Spin-orbit  
force  
predicted!**

**Note the totally new, subtle density dependence**



# First systematic approach to finite nuclei

J.R. Stone, P.A.M. Guichon, P. G. Reinhard & A.W. Thomas  
( Phys Rev Lett, 116 (2016) 092501 )

- **Constrain 3 basic quark-meson couplings ( $g_{\sigma}^q, g_{\omega}^q, g_{\rho}^q$ ) so that nuclear matter properties are reproduced within errors**

$$-17 < E/A < -15 \text{ MeV}$$

$$0.14 < \rho_0 < 0.18 \text{ fm}^{-3}$$

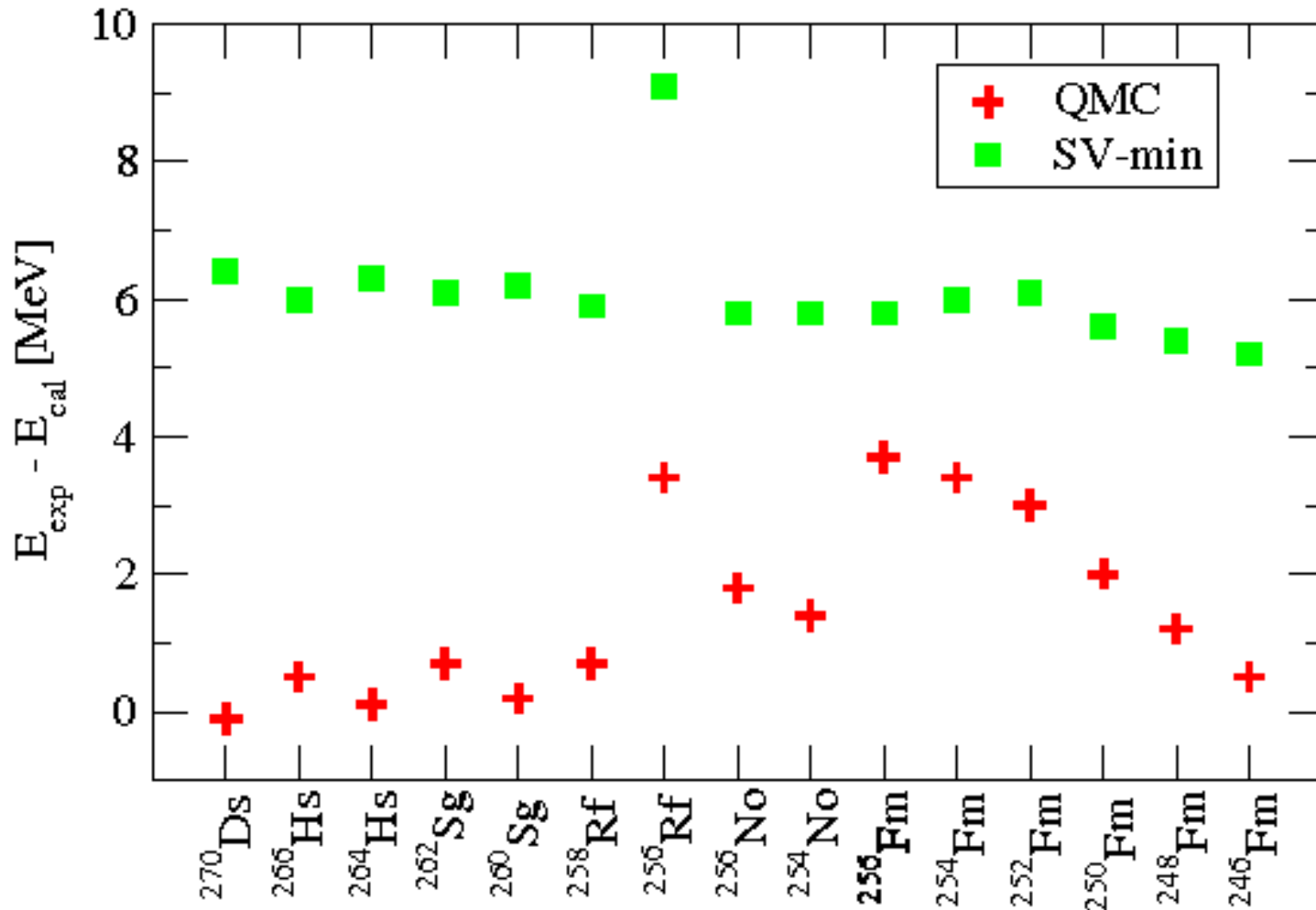
$$28 < S_0 < 34 \text{ MeV}$$

$$L > 20 \text{ MeV}$$

$$250 < K_0 < 350 \text{ MeV}$$

- **Fix at overall best description of finite nuclei with 5 parameters ( 3 for the EDF +2 pairing pars)**
- **Benchmark comparison: SV-min 16 parameters (11+5 pairing)**

# Superheavies not fit: 0.1% accuracy



Stone et al., PRL 116 (2016) 092501

For detailed study of SHE see: [arXiv:1901.06064](https://arxiv.org/abs/1901.06064)

# Latest Nuclear Structure Results

Includes some unpublished results for QMC  $\pi$ -III from

PhD thesis of Kay Martinez

- now at Silliman University (Philippines)  
(publications in preparation)

- in collaboration with Pierre Guichon and Jirina Stone

QMC  $\pi$ -II and III incorporate a much more  
accurate evaluation of  $H^\sigma$

# QMC $\pi$ -III

- **Just 5 parameters\***:  $m_\sigma$ , quark couplings to  $\sigma$ ,  $\omega$  and  $\rho$  mesons and  $\lambda_3$  - the strength of  $\sigma^3$  term

- Tensor term included:
 
$$H_{\sigma,\omega,\rho}^J = \left( \frac{G_\sigma(1-dv_0)^2}{4m_\sigma^2} - \frac{G_\omega}{4m_\omega^2} \right) \sum_m \vec{J}_m^2 - \frac{G_\rho}{4m_\rho^2} \sum_{m,m'} S_{m,m'} \vec{J}_m \cdot \vec{J}_{m'},$$

and

$$H_S^J = -\frac{G_\sigma - G_\omega}{16M^2} \sum_m \vec{J}_m^2 + \frac{G_\rho}{16M^2} \sum_{mm'} S_{m,m'} \vec{J}_m \cdot \vec{J}_{m'}.$$

with

$$\vec{J}_m = i \sum_{i \in F_m} \sum_{\sigma\sigma'} \vec{\sigma}_{\sigma'\sigma} \times [\vec{\nabla} \phi^i(\vec{r}, \sigma, m)] \phi^{i*}(\vec{r}, \sigma', m), \quad \vec{J} = \vec{J}_p + \vec{J}_n,$$

- Pairing interaction (simple BCS) derived in the model

$$V_{\text{pair}}^{\text{QMC}} = - \left( \frac{G_\sigma}{1 + d' G_\sigma \rho(\vec{r})} - G_\omega - \frac{G_\rho}{4} \right) \delta(\vec{r} - \vec{r}')$$

$$d' = d + \frac{1}{3} G_\sigma \lambda_3,$$

\*cf. Over 25 in FRDM and typically 16 (11+5) in Skyrme forces

# Giant Monopole Resonances

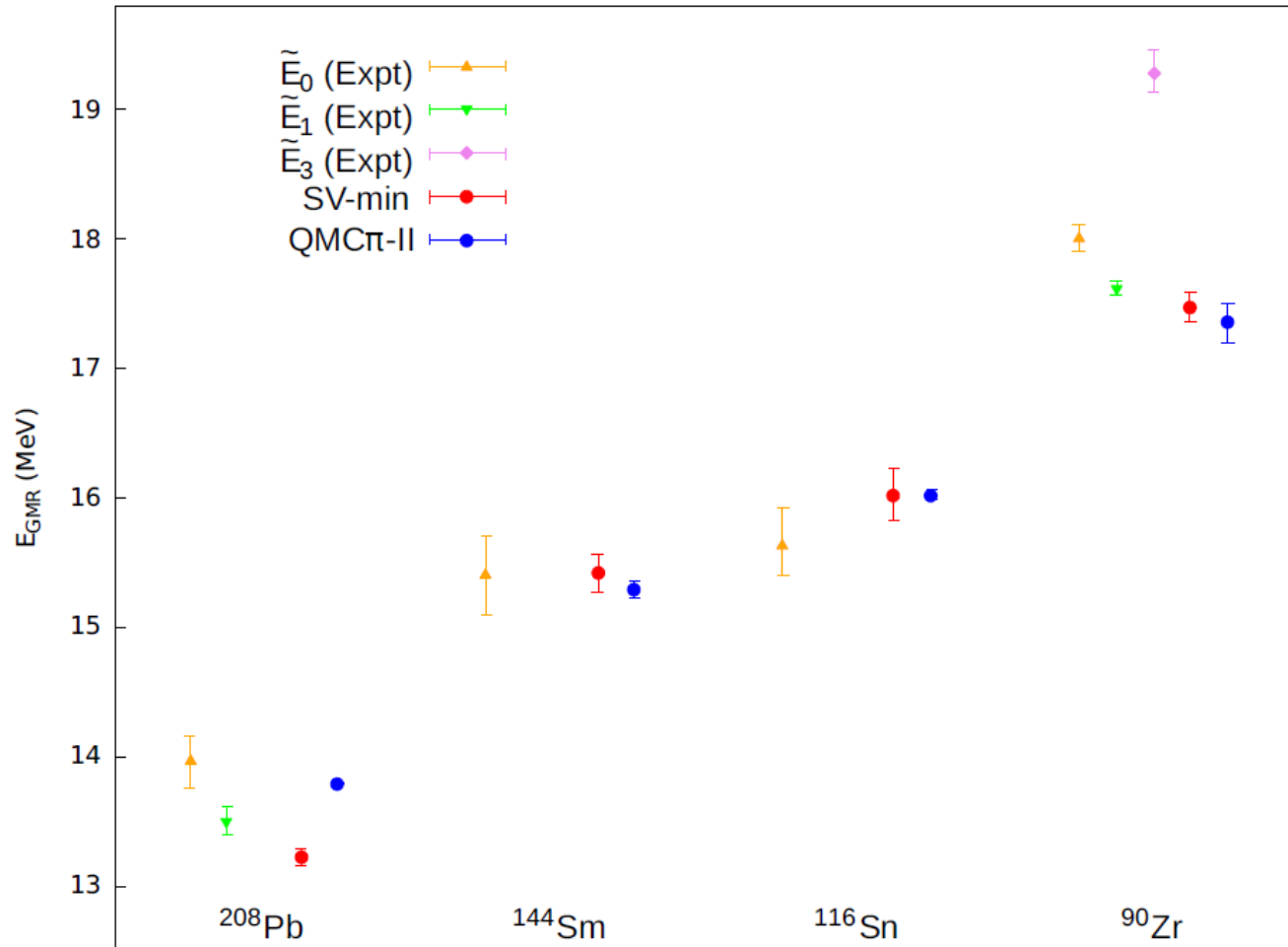
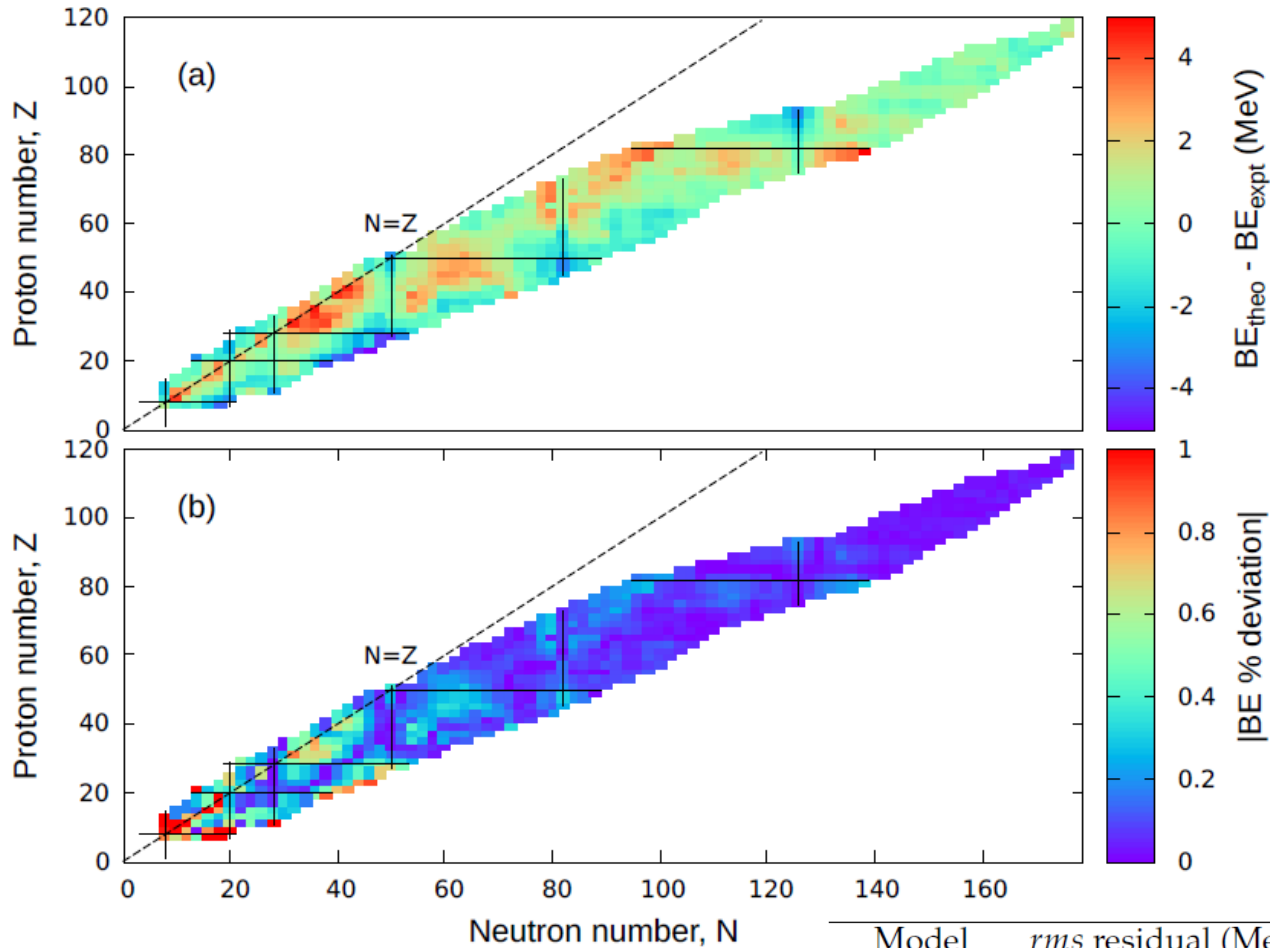


FIG. 13. GMR energies for  $^{208}\text{Pb}$ ,  $^{144}\text{Sm}$ ,  $^{116}\text{Sn}$ , and  $^{90}\text{Zr}$  from experiment and for the QMC $\pi$ -II and SVmin models. Experimental data are taken from Table 1 of Ref. [24].

This required the introduction of a term  $\sim\lambda_3\sigma^3$   
Kay Martinez *et al.*, Phys Rev C100 (2019) 024333

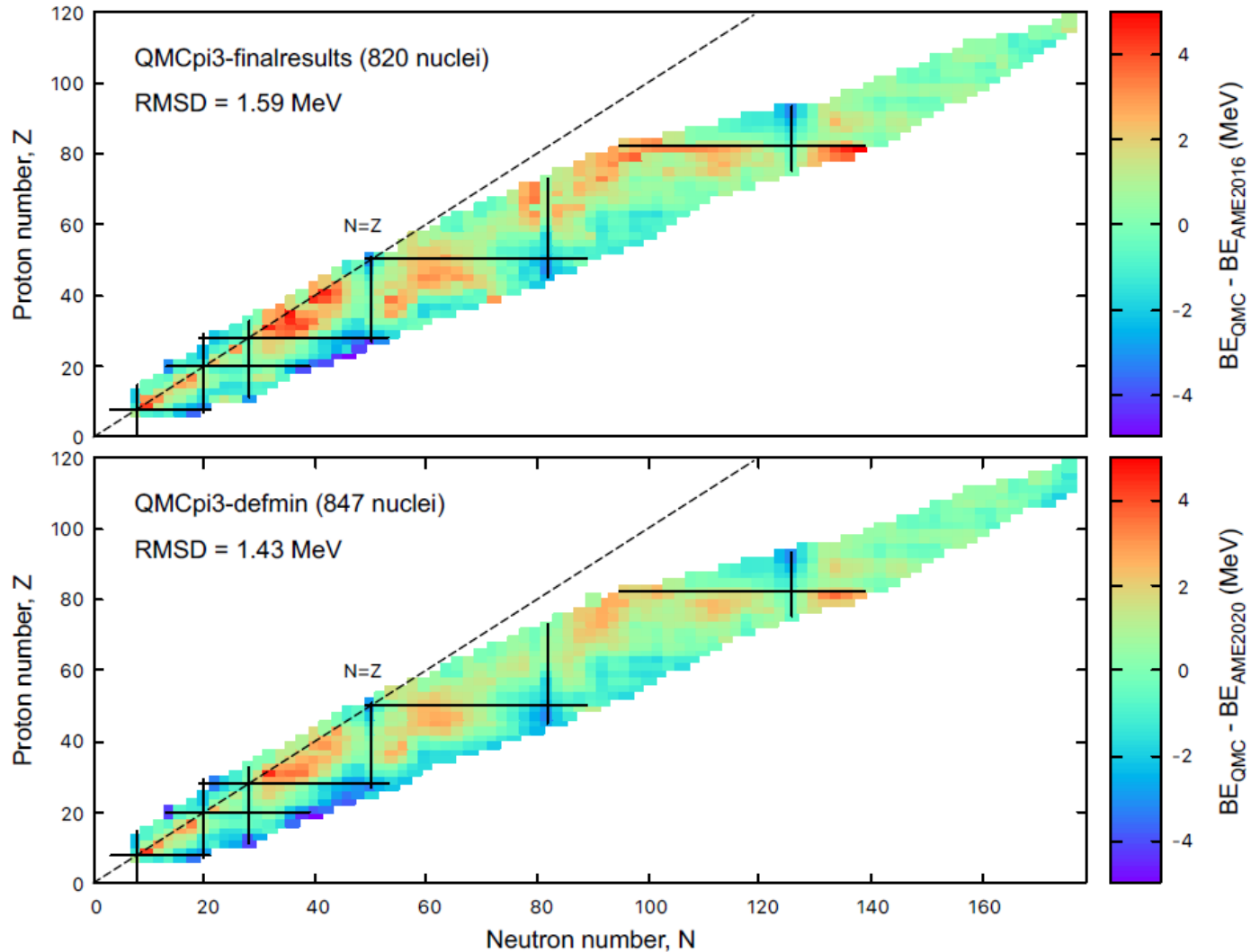
# Binding Energies – 820 Known Even-Even Nuclei

2020



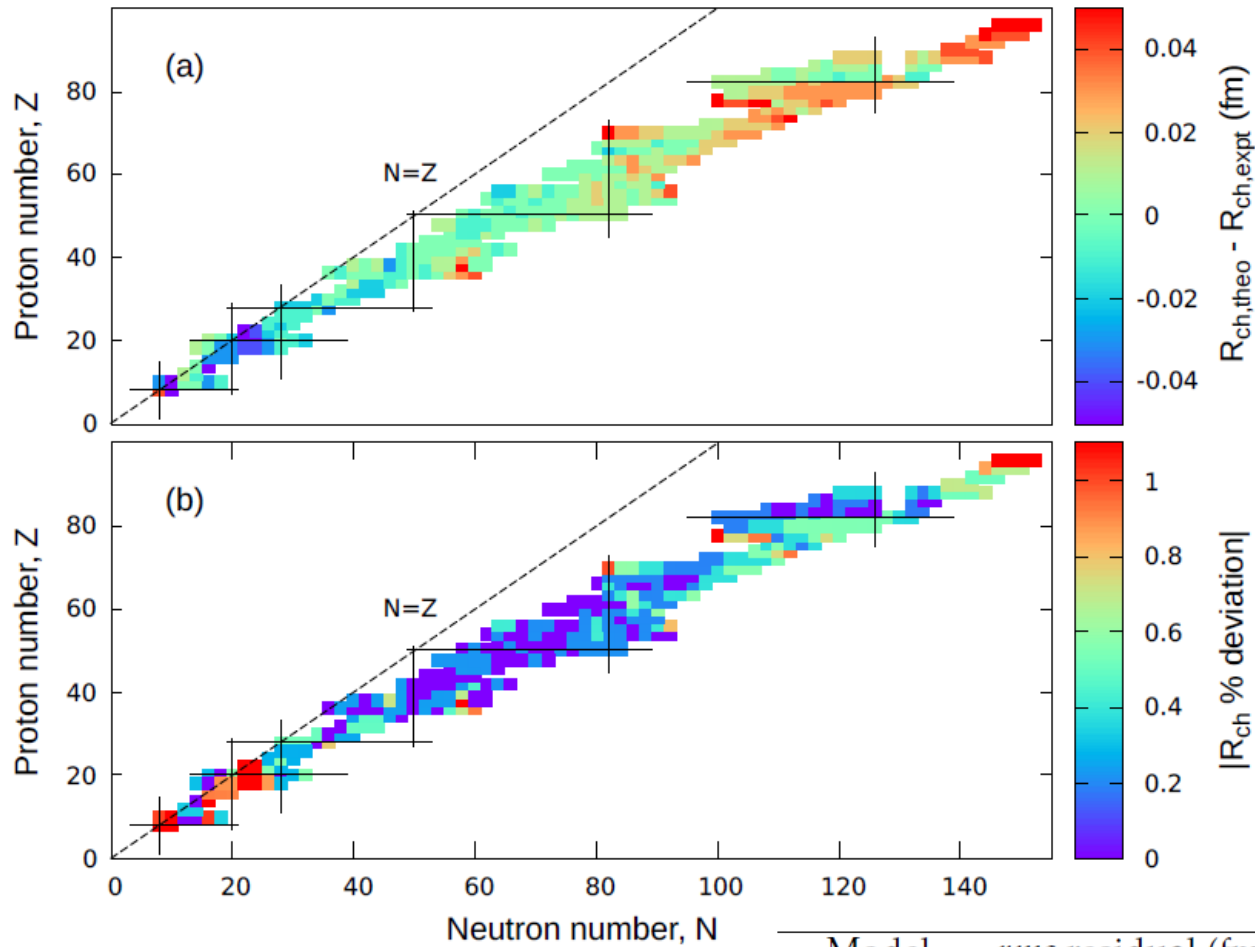
Model	<i>rms</i> residual (MeV)	<i>rms</i> % deviation
QMC $\pi$ -III	1.59	0.29
QMC $\pi$ -II	2.34	0.39
QMC $\pi$ -I	2.78	0.50
QMC-I	3.84	0.69
SV-min	3.64	0.38
UNEDF1	2.06	0.55
DD-ME $\delta$	2.41	0.42
FRDM	0.89	0.18

# Latest analysis: data from Atomic Mass Evaluation 2020



2023

# Charge Radii



Model	<i>rms</i> residual (fm)	<i>rms</i> % deviation
QMC $\pi$ -III	0.024	0.50
QMC $\pi$ -II	0.029	0.66
QMC $\pi$ -I	0.028	0.65
QMC-I	0.030	0.66
SV-min	0.024	0.61
UNEDF1	0.029	0.65
DD-ME $\delta$	0.035	0.78



# Separation energies: Drip Lines

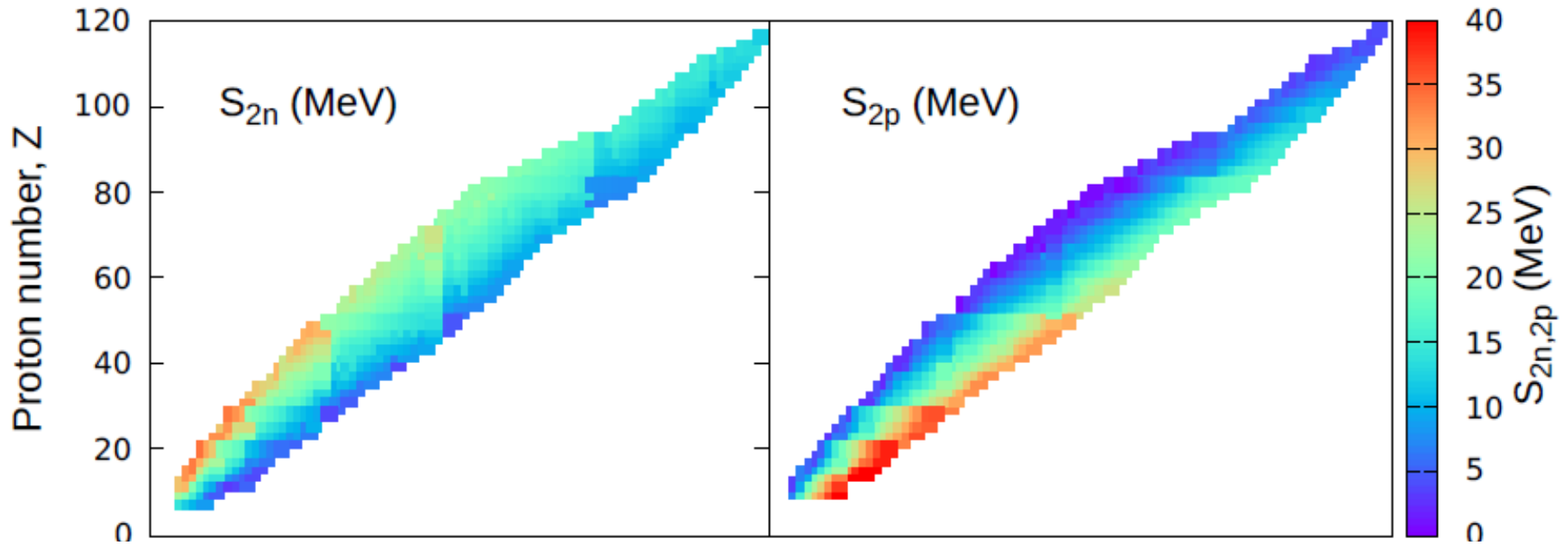
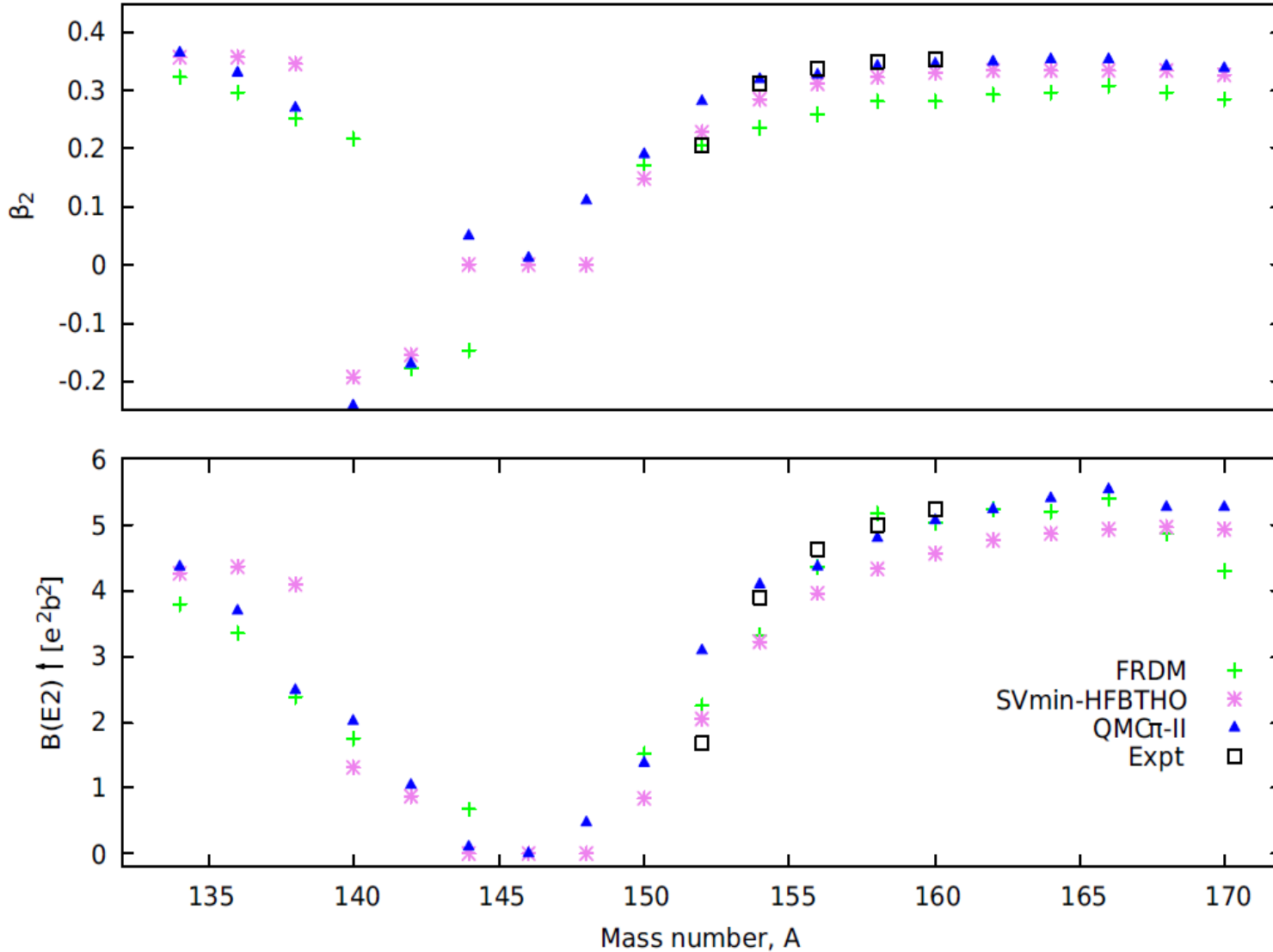


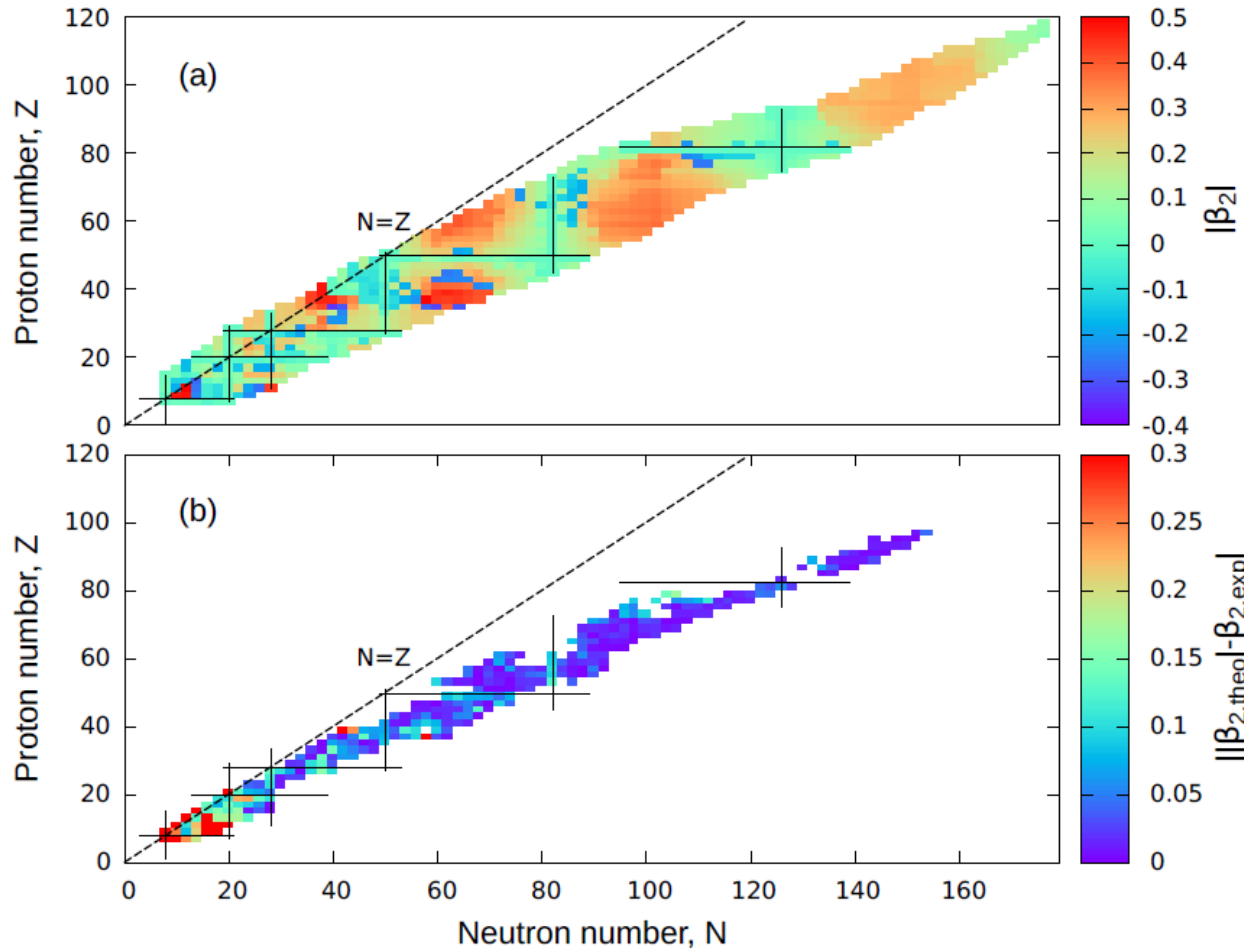
TABLE 7.3: Comparison of *rms* residuals for separation energies (in MeV) from QMC and from other nuclear models.

Model	$S_{2n}$	$S_{2p}$	$\delta_{2n}$	$\delta_{2p}$
QMC $\pi$ -III	0.97	0.95	1.24	1.28
QMC $\pi$ -II	1.03	1.08	1.20	1.25
SV-min	0.77	0.82	0.87	1.00
UNEDF1	0.74	0.82	0.85	0.90
DD-ME $\delta$	1.01	1.05	1.12	1.11
FRDM	0.50	0.55	0.61	0.75

# Deformation of Gd isotopes



# Deformation



Model	<i>rms</i> residual	<i>rms</i> % deviation
QMC $\pi$ -III	0.11	28
SV-min	0.16	59
UNEDF1	0.15	53
DD-ME $\delta$	0.14	40
FRDM	0.11	30

# The Superheavy Region

## First study in QMC:

PHYSICAL REVIEW C **100**, 044302 (2019)

---

### Physics of even-even superheavy nuclei with $96 < Z < 110$ in the quark-meson-coupling model

J. R. Stone\*

*Department of Physics (Astro), University of Oxford, Keble Road OX1 3RH, Oxford, United Kingdom  
and Department of Physics and Astronomy, University of Tennessee, Knoxville, Tennessee 37996, USA*

K. Morita†

*Department of Physics, Kyushu University, Nishi-ku, Fukuoka 819-0395, Japan  
and RIKEN Nishina Center, RIKEN, Wako-shi, Saitama 351-0198, Japan*

P. A. M. Guichon‡

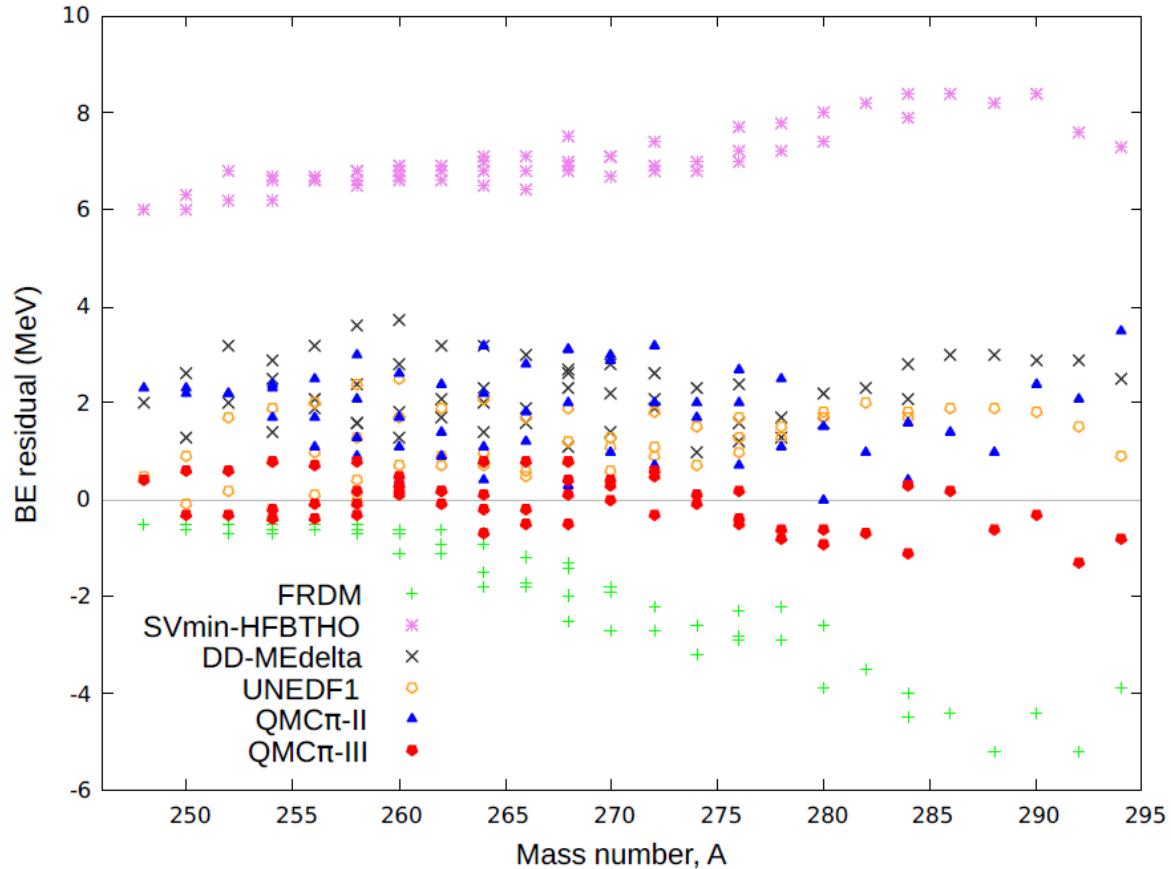
*CEA/IRFU/SPhN Saclay, F91191, France*

A. W. Thomas§

*CSSM and CoEPP, Department of Physics, University of Adelaide, SA 5005, Australia*

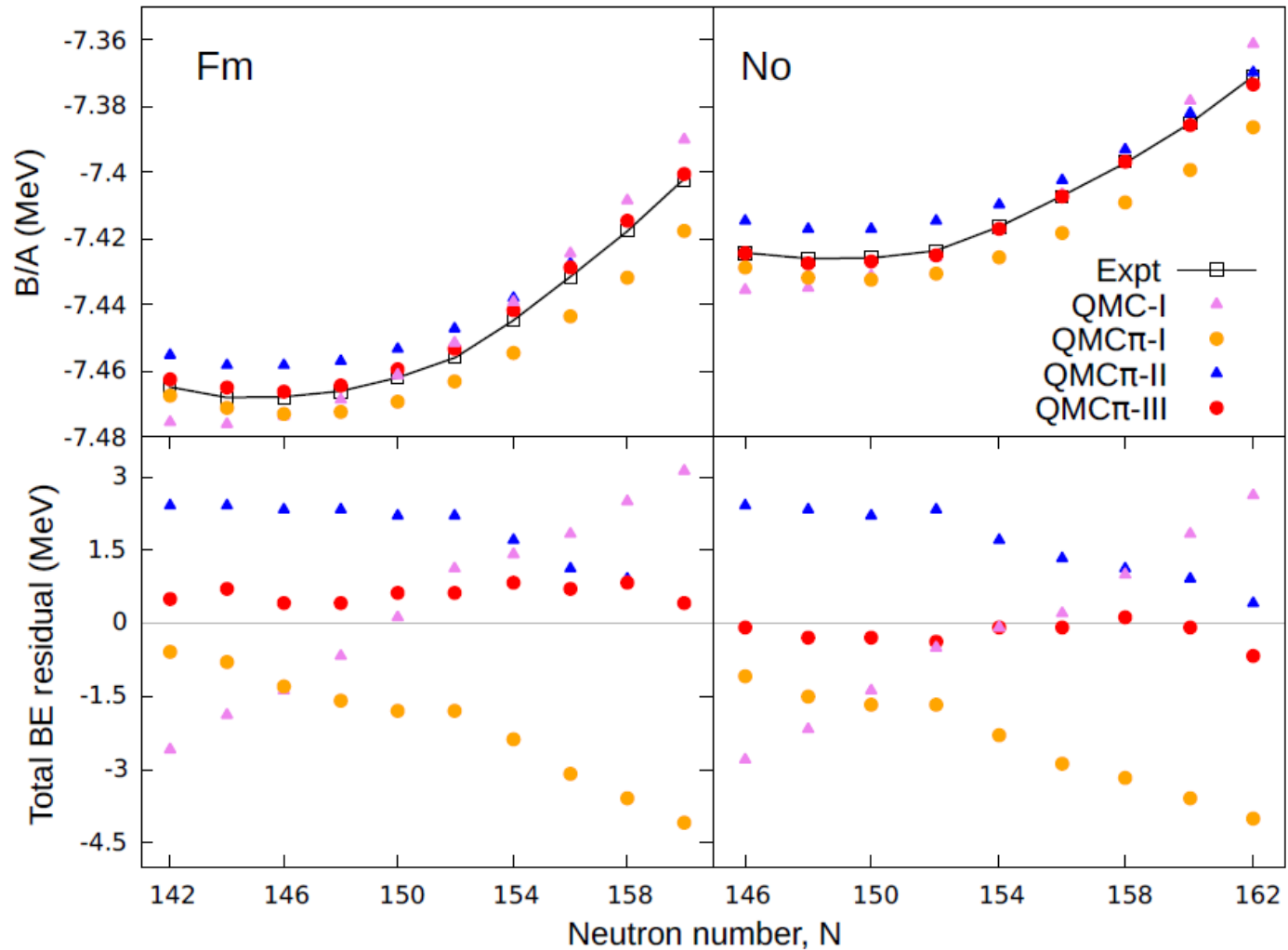
**Updated and expanded here (Martinez thesis)**

# Binding Energies

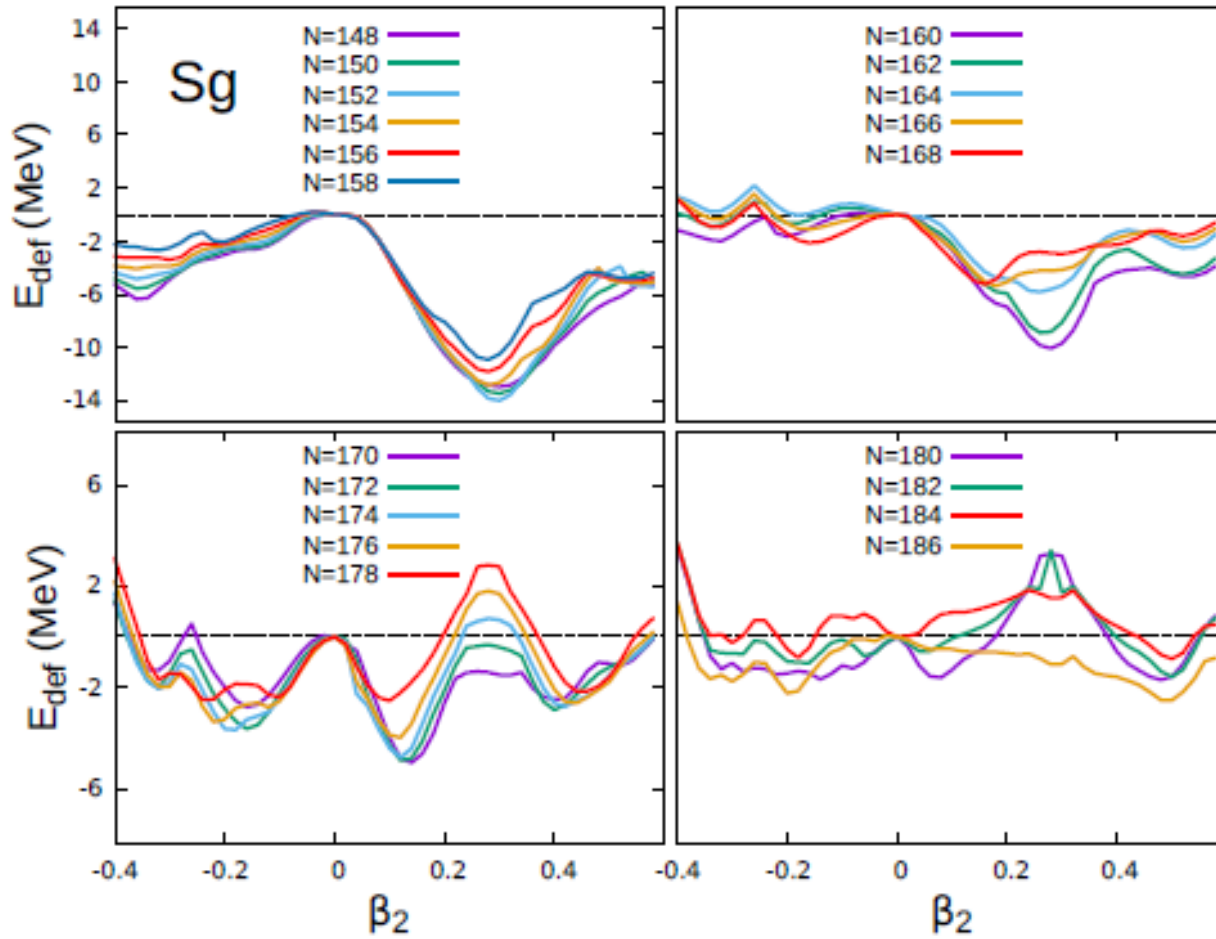


	<i>rms</i> % deviation	<i>rms</i> residual (MeV)	
QMC $\pi$ -III	0.03	0.52	<b>Outstanding agreement</b>
QMC $\pi$ -II [54]	0.11	2.04	
QMC $\pi$ -I [53]	0.12	2.42	
QMC-I [8]	0.08	1.50	
FRDM [23]	0.11	2.25	
SV-min [24]	0.36	6.99	
UNEDF1 [28]	0.07	1.31	
DD-ME $\delta$ [66]	0.12	2.28	

# Trends Along Chains: $^{100}\text{Fm}$ and $^{102}\text{No}$



# Many Almost Degenerate Minima in Superheavy Region



# Hypernuclei

No new parameters as  $\sigma$ ,  $\omega$  and  $\rho$  mesons do not couple to the strange quark.

One could add extra mesons with more free parameters but let's see what we find.....



# $\Lambda$ - and $\Xi$ -Hypernuclei in QMC

	$^{89}_{\Lambda}\text{Yb}$ (Expt.)	$^{91}_{\Lambda}\text{Zr}$	$^{91}_{\Xi^0}\text{Zr}$	$^{208}_{\Lambda}\text{Pb}$ (Expt.)	$^{209}_{\Lambda}\text{Pb}$	$^{209}_{\Xi^0}\text{Pb}$
$1s_{1/2}$	-22.5	-24.0	-9.9	-27.0	-26.9	-15.0
$1p_{3/2}$		-19.4	-7.0		-24.0	-12.6
$1p_{1/2}$	-16.0 (1p)	-19.4	-7.2	-22.0 (1p)	-24.0	-12.7
$1d_{5/2}$		-13.4	-3.1	—	-20.1	-9.6
$2s_{1/2}$		-9.1	—	—	-17.1	-8.2
$1d_{3/2}$	-9.0 (1d)	-13.4	-3.4	-17.0 (1d)	-20.1	-9.8
$1f_{7/2}$		-6.5	—	—	-15.4	-6.2
$2p_{3/2}$		-1.7	—	—	-11.4	-4.2
$1f_{5/2}$	-2.0 (1f)	-6.4	—	-12.0 (1f)	-15.4	-6.5
$2p_{1/2}$		-1.6	—	—	-11.4	-4.3

Also predicts  $\Xi$  – hypernuclei bound by 5-15 MeV – being tested at J-PARC

“The first evidence of a bound state of  $\Xi^{-14}\text{N}$  system”,

K. Nakazawa et al.,

Prog. Theor. Exp. Phys. (2015)

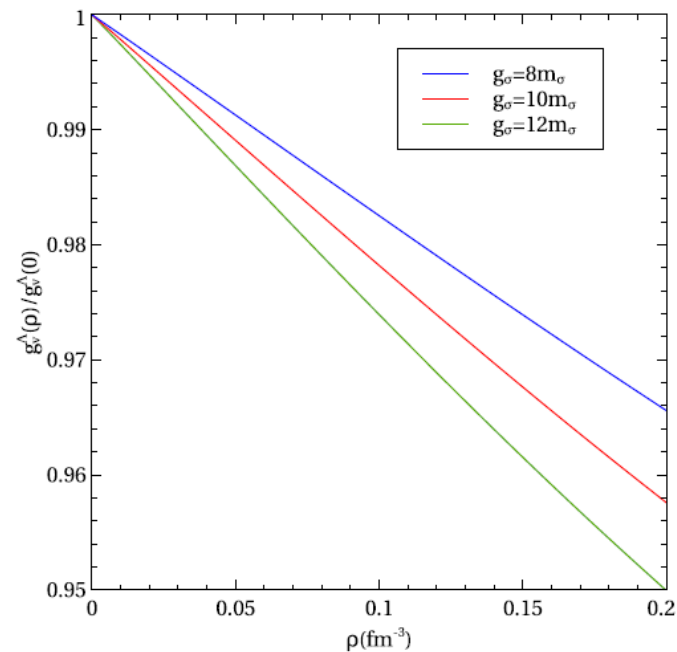
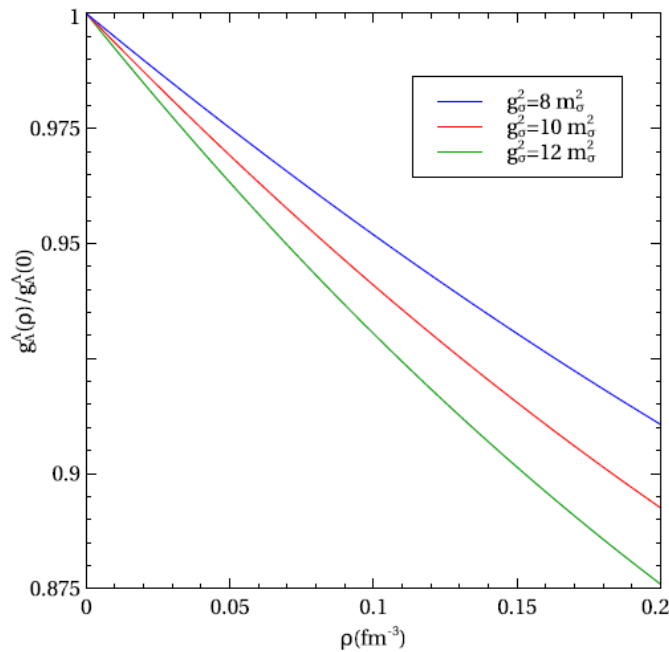
Guichon et al., Nucl.Phys. A814 (2008) 66; see also 1998

**At the heart of this approach is the change in baryon structure in-medium**

**This needs to be tested and hypernuclei offer a great deal of promise**

# Change in Structure of Bound $\Lambda$

- Effect of the  $\sigma$  mean field is to modify the wave functions of the light quarks in the N
- Hence, the rates of vector and axial vector strangeness changing weak decays change in-medium
  - calculation respects Ademollo-Gatto Theorem



Guichon & Thomas, Phys Lett B773 (2017) 332

## Experiments to investigate possible modification of baryons in nuclear matter

- Magnetic moment of  $\Lambda$  in nuclei via  $B(M1)$  of  $\Lambda$ 's spin-flip transition ( ${}^7_{\Lambda}\text{Li}$ ) (J-PARC E63, approved, under preparation)
- Beta-decay rate of  $\Lambda$  in nuclei ( ${}^5_{\Lambda}\text{He}$  or  ${}^4_{\Lambda}\text{H}$ ) (LOI submitted to J-PARC, under designing the experiment)
- Magnetic moment of  $\Sigma$  in nuclei ( ${}^4_{\Sigma}\text{He}$ )

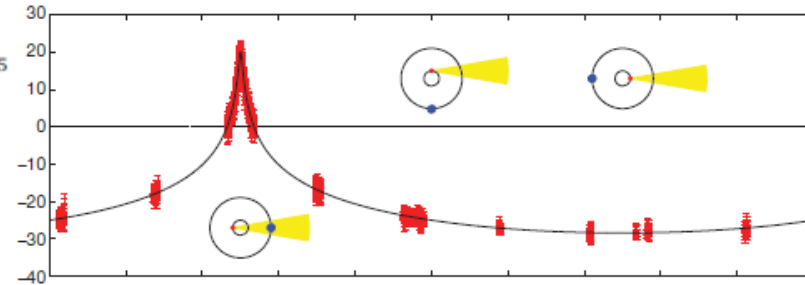
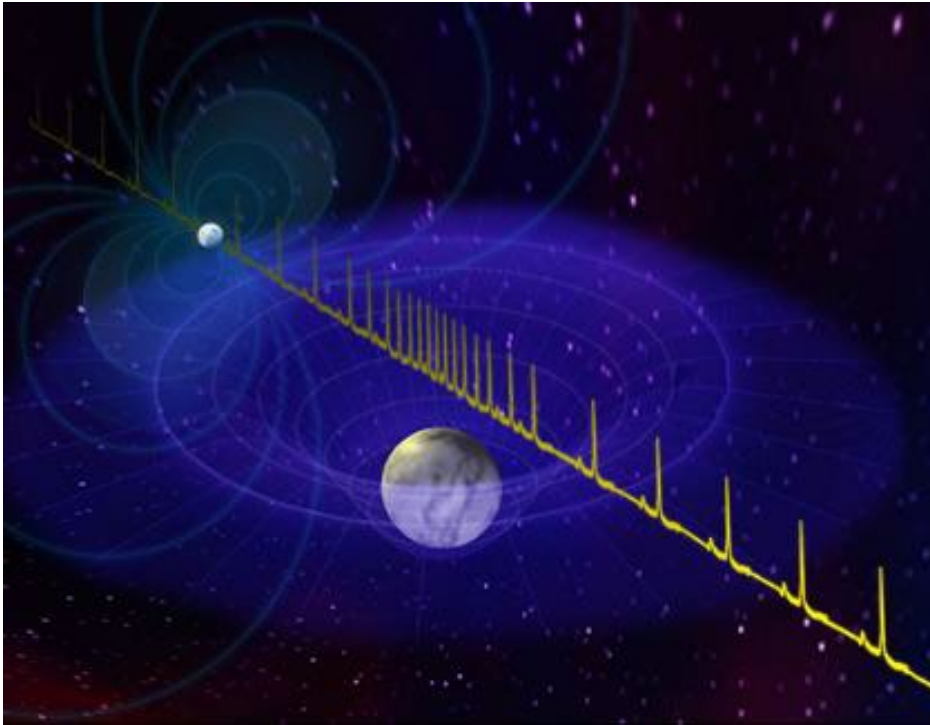
In response to the last issue a preliminary calculation of the  $\Sigma^0 \rightarrow \Lambda\gamma$  M1 decay for a  $\Sigma^0$  bound by 7.6 MeV in  ${}^4_{\Sigma}\text{He}$  yields  $\Delta\Gamma_{M1}(\Sigma \rightarrow \Lambda\gamma)$  of order 12%



# Neutron Stars

# A two-solar-mass neutron star measured using Shapiro delay

P. B. Demorest<sup>1</sup>, T. Pennucci<sup>2</sup>, S. M. Ransom<sup>1</sup>, M. S. E. Roberts<sup>3</sup> & J. W. T. Hessels<sup>4,5</sup>



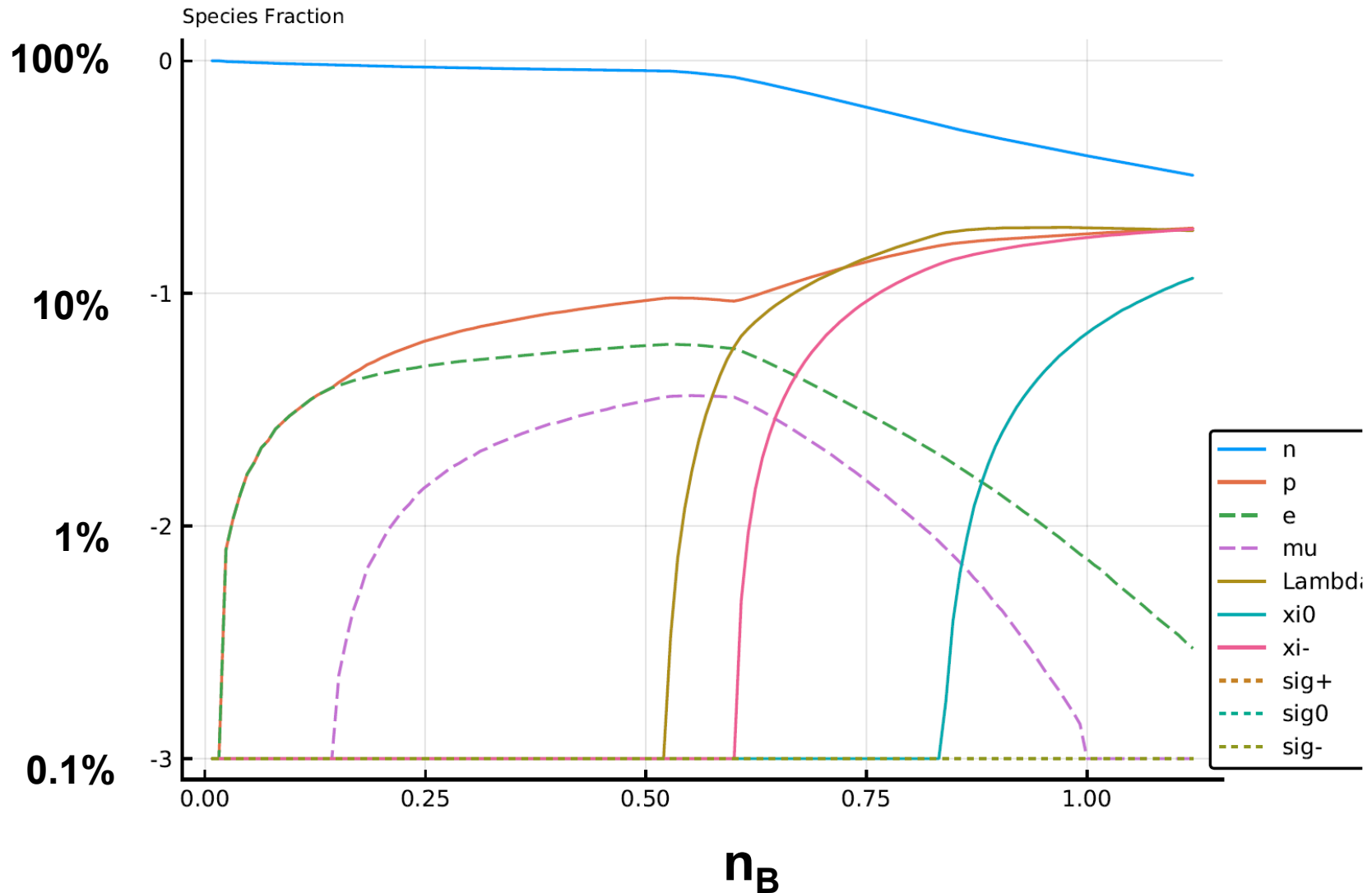
Reported a very accurate pulsar mass much larger than seen before :  $1.97 \pm 0.04$  solar mass

Claim: it rules out hyperon occurrence

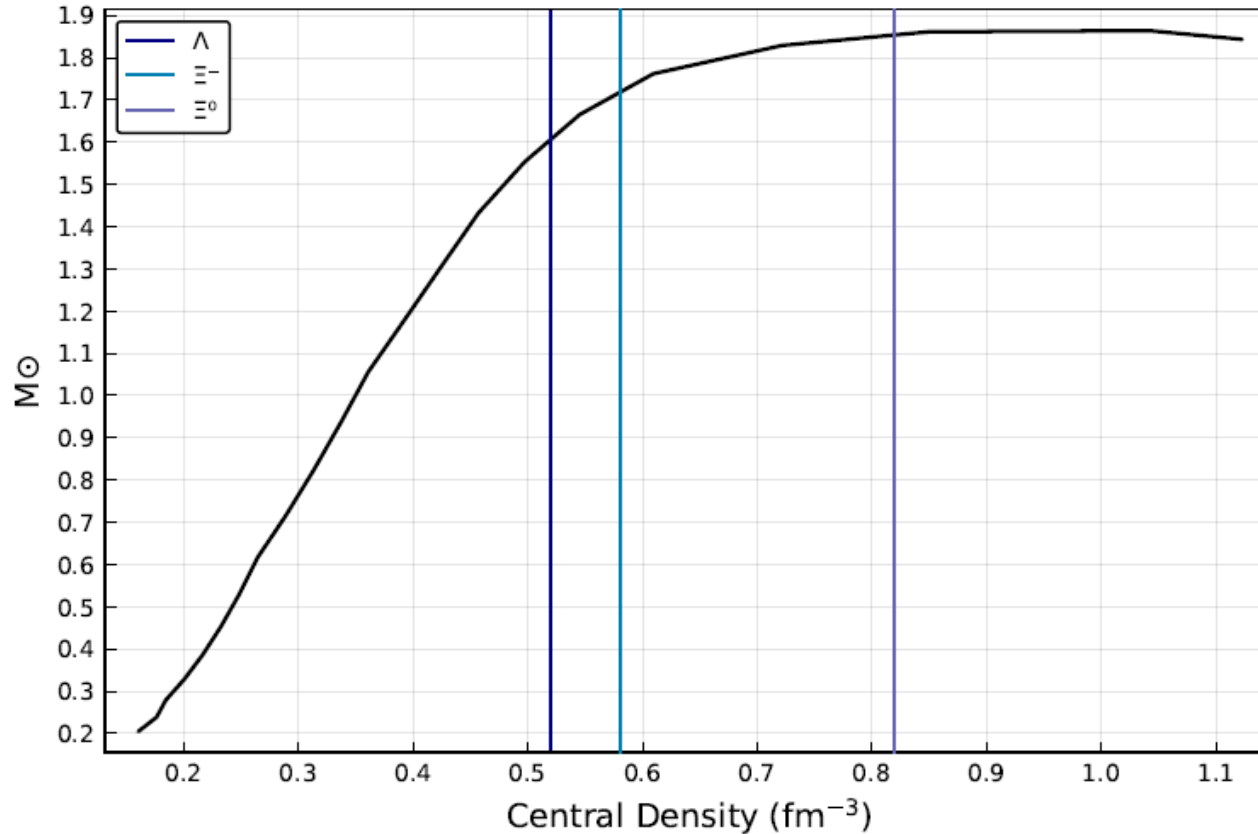
- ignored our work *published* three years before!

Rikovska-Stone *et al.*, NP A792 (2007) 341

# Species Fractions: in $\beta$ -equilibrium

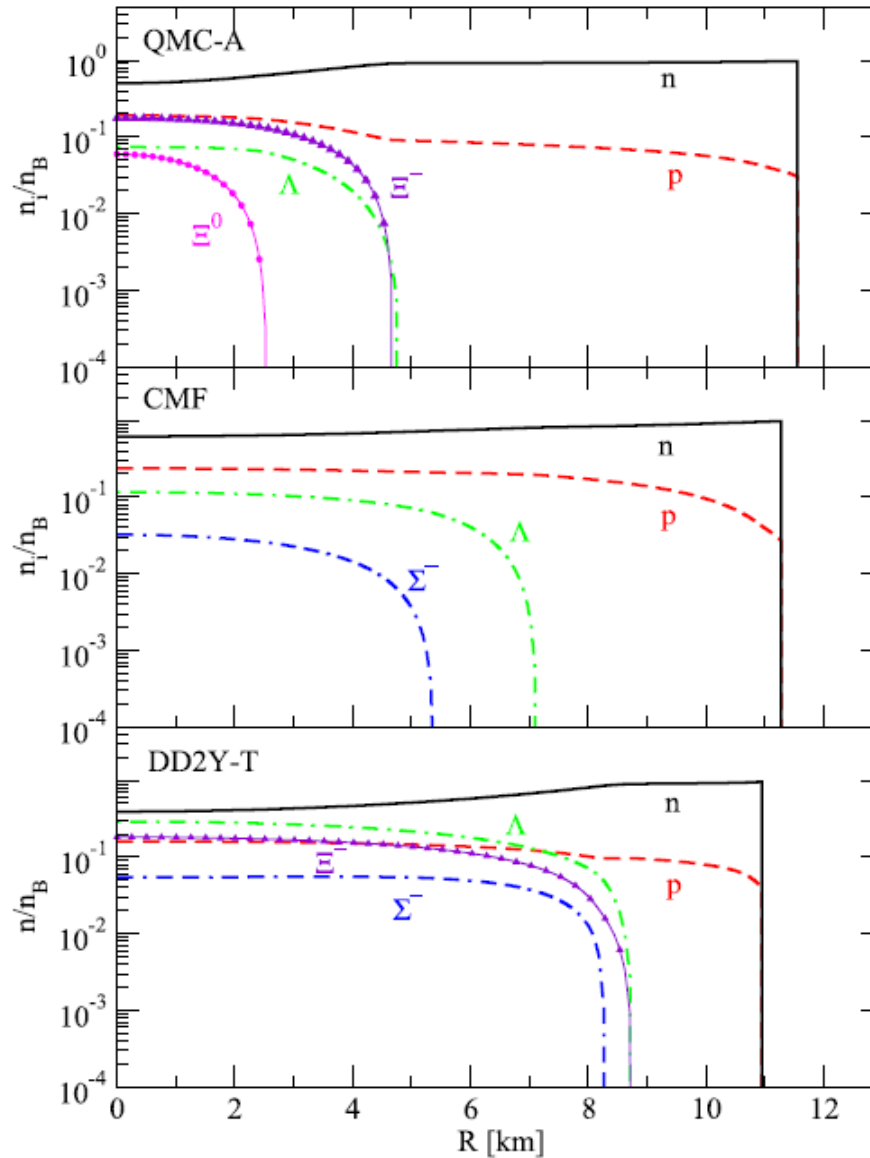


# Hadron Content versus NS Mass

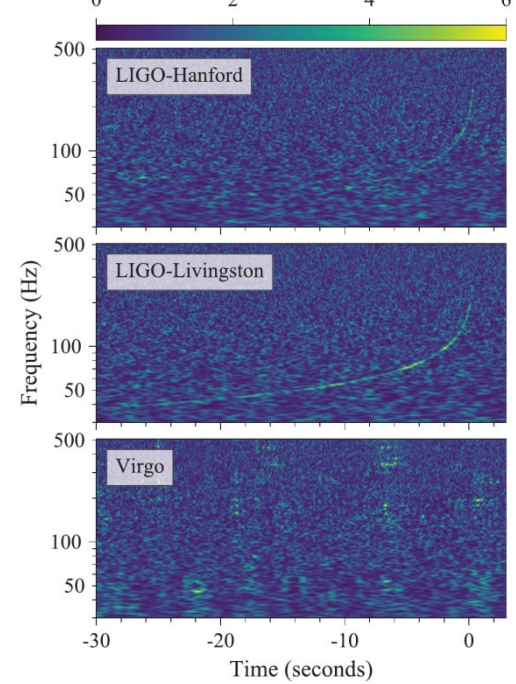




# Radial Distribution of Hyperons (T=0)



Stone *et al.*, *MNRAS* 502, 3476–3490 (2021)



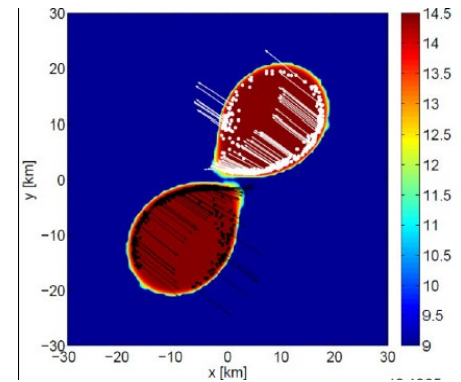
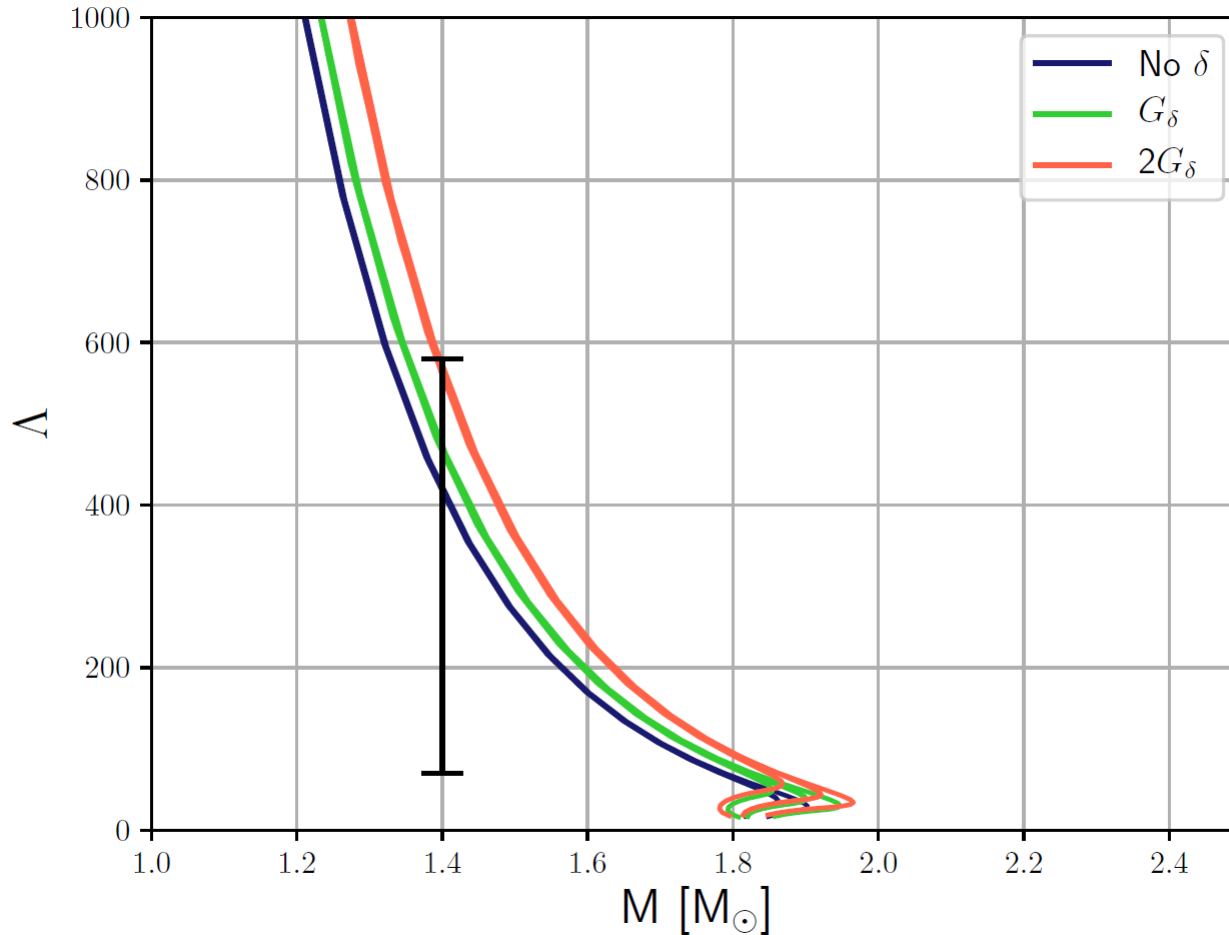
# GW170817: Measurements of neutron star radii and equation of state

The LIGO Scientific Collaboration and The Virgo Collaboration  
( compiled 30 May 2018)

On August 17, 2017, the LIGO and Virgo observatories made the first direct detection of gravitational waves from the coalescence of a neutron star binary system. The detection of this gravitational wave signal, GW170817, offers a novel opportunity to directly probe the properties of matter at the extreme conditions found in the interior of these stars. The initial, minimal-assumption analysis of the LIGO and

# Tidal deformability

- Band deduced by LIGO-Virgo analysis of GW170817



$$Q_{ij} = -\lambda(M) E_{ij}$$

# Finite Temperature

As we have heard at this meeting (e.g. Perego and Kochankovski ) after BNS mergers the temperature in time-frame relevant to Gravitational Waves is 10-100 MeV

The composition is then very different from a cold star

For example,  $\Sigma$  hyperons which play no role in QMC at  $T=0$  because of the enhancement of the color hyperfine repulsion play an important role

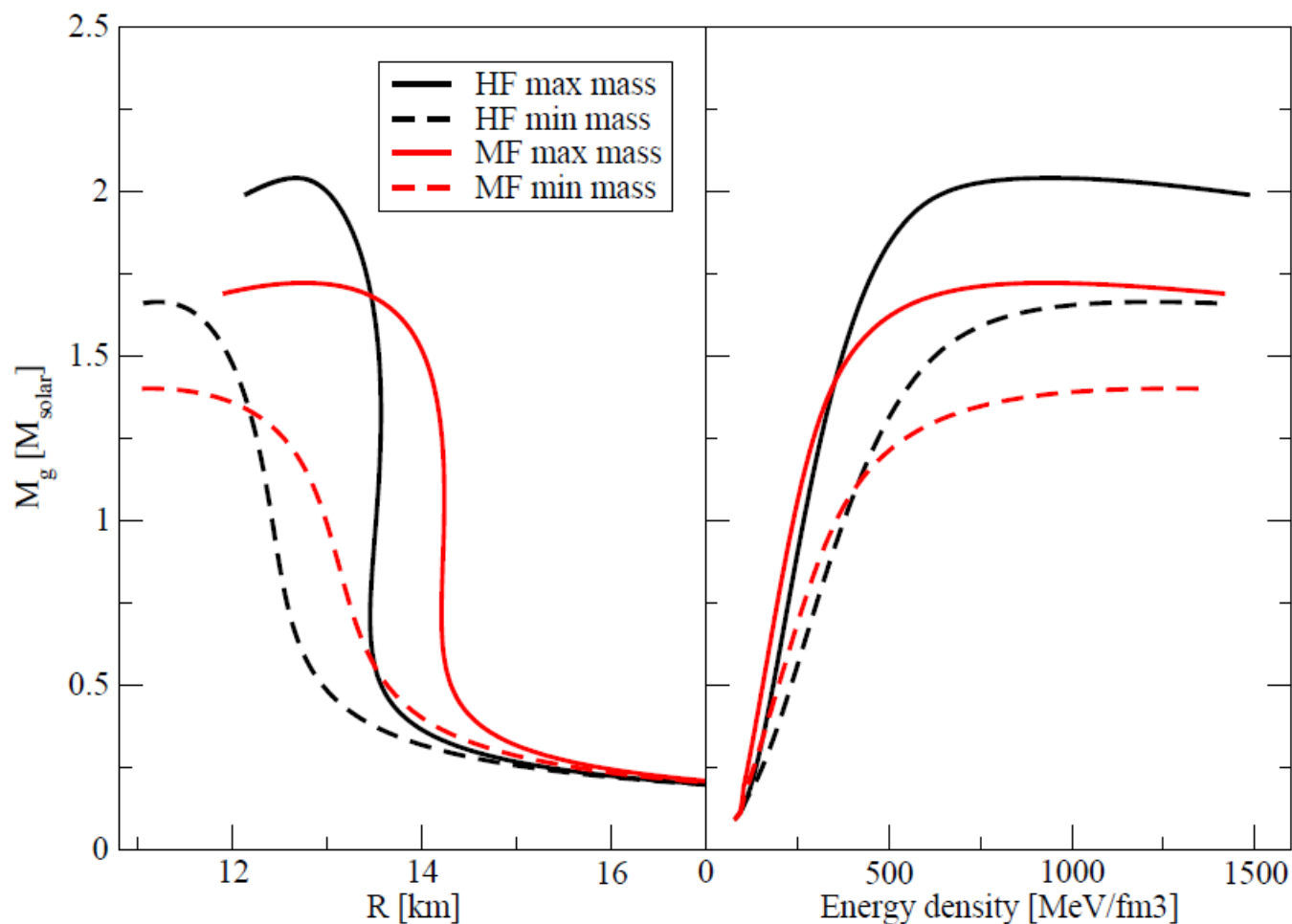
See:

Stone *et al.*, [MNRAS 502, 3476–3490 \(2021\)](#)

and Guichon *et al.*, to appear within a week...

# Relativistic Hartree-Fock vs RMF

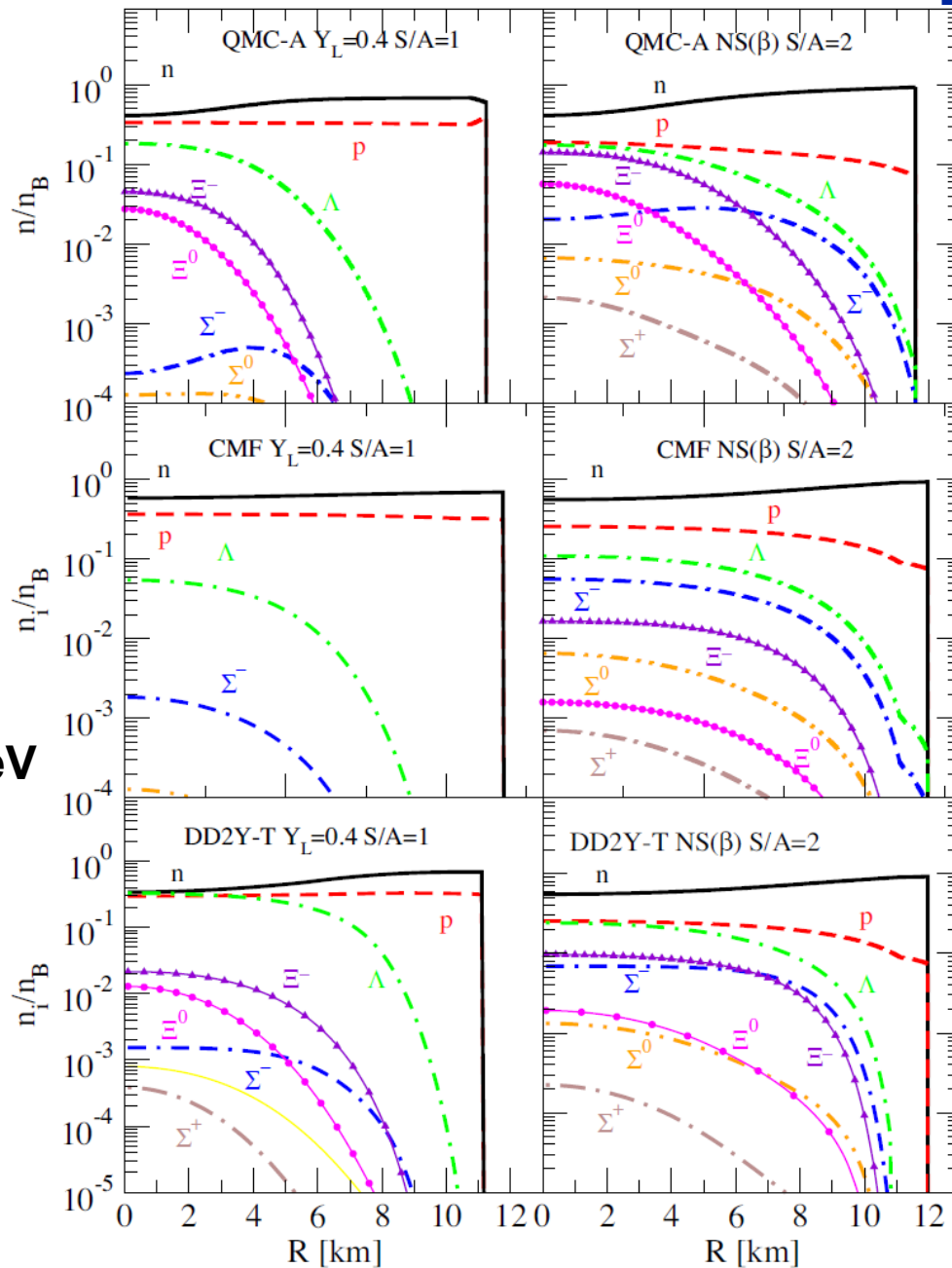
Upper and lower limits vs nuclear matter parameters:



# Hyperon content at finite Temperature

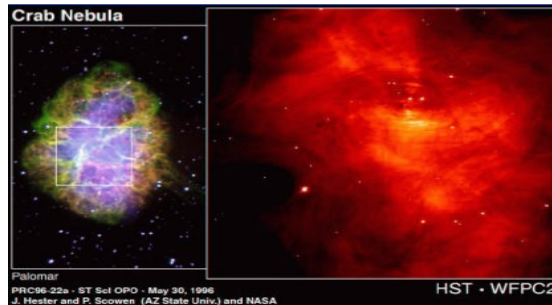
**T = 10-20 MeV**

**T = 20-40 MeV**



# Summary

- Intermediate range NN attraction is **STRONG** Lorentz scalar
- This modifies the intrinsic structure of the bound nucleon
  - profound change in shell model :  
what occupies shell model states are **NOT** free nucleons
- Scalar polarizability is a natural source of three-body forces (NNN, HNN, HHN...)
  - clear physical interpretation
- Naturally generates effective HN and HNN forces with no new parameters and predicts heavy neutron stars



# Summary

- **Need empirical confirmation of changing baryon structure:**
  - Response Functions & Coulomb sum rule
  - EMC effect; spin EMC (not too long...)
  - Change in  $\Lambda$  decay rate in nuclei?
  - $\Delta\Gamma_{M1}(\Sigma \rightarrow \Lambda\gamma)$  in  ${}^4_{\Sigma}\text{He}$
- **Initial systematic study of finite nuclei very promising**  
**With just 5 parameters:**
  - Binding energies typically within 0.29% across periodic table
  - Super-heavies ( $Z > 100$ ) especially good: 0.03%
  - Systematics of charge radii, deformations, shell and subshell closures pretty good



# Special Mentions.....



**Guichon**



**Tsushima**



**Saito**



**Stone**



**Krein**



**Matevosyan**



**Cloët**



**Whittenbury**



**Simenel**



**Bentz**



**Martinez**



**Motta**



**Antic**



**Kalaitzis**

**P. G. Reinhard  
Skyax**



# Suggests a different approach: QMC Model

(Guichon 1988, Guichon, Saito, Tsushima et al., Rodionov et al., Stone - see Saito *et al.*, Prog. Part. Nucl. Phys. 58 (2007) 1 and Guichon *et al.*, Prog. Part. Nucl. Phys. 100 (2018) 262-297 for reviews)

- Start with quark model (MIT bag/NJL...) for all hadrons

- Introduce a relativistic Lagrangian with  $\sigma$ ,  $\omega$  and  $\rho$  mesons coupling to non-strange quarks

- Hence, initially only 4 parameters

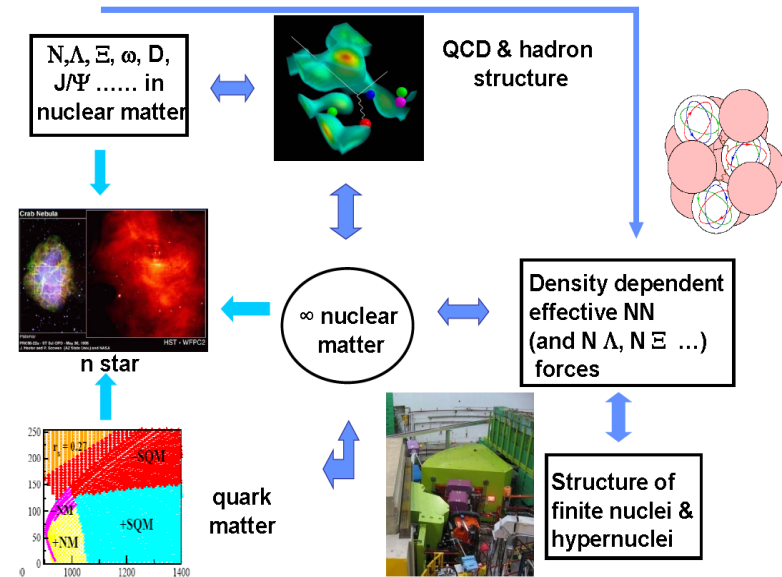
$$(m_\sigma, g^{\sigma, \omega, \rho}_q)$$

– determine by fitting to:

$\rho_0$ ,  $E/A$  and symmetry energy

– same in dense matter & finite nuclei

- Must solve self-consistently for the internal structure of baryons in-medium



# 2016: Overview of 106 Nuclei Studied – Across Periodic Table

Element	Z	N	Element	Z	N
C	6	6 -16	Pb	82	116 - 132
O	8	4 -20	Pu	94	134 - 154
Ca	20	16 - 32	Fm	100	148 - 156
Ni	28	24 - 50	No	102	152 - 154
Sr	38	36 - 64	Rf	104	152 - 154
Zr	40	44 -64	Sg	106	154 - 156
Sn	50	50 - 86	Hs	108	156 - 158
Sm	62	74 - 98	Ds	110	160
Gd	64	74 -100			

Not  
fit

N	Z	N	Z
20	10 - 24	64	36 - 58
28	12 - 32	82	46 - 72
40	22 - 40	126	76 - 92
50	28 - 50		

i.e. We look at most challenging cases of p- or n-rich nuclei

Recall that in QMC $\pi$ -II we write the  $\sigma$  field as  $\sigma = \bar{\sigma} + \delta\sigma$ , which naturally leads to a classical mean part of the  $\sigma$  field Hamiltonian,  $H_{\text{mean}}^\sigma$  and a fluctuation part  $H_{\text{fluc}}^\sigma$ . The effective QMC nucleon mass is expressed as before, as  $M_{\text{QMC}}(\bar{\sigma}) = M - g_\sigma \bar{\sigma} + \frac{d}{2}(g_\sigma \bar{\sigma})^2$ , where  $g_\sigma$  is the coupling of the nucleon to the  $\sigma$  meson in free space,  $d$  is the scalar polarizability, and the classical  $\sigma$  field satisfies the wave equation,

$$-\nabla^2 \bar{\sigma} + \frac{dV(\bar{\sigma})}{d\bar{\sigma}} = -\left\langle \frac{\partial K}{\partial \bar{\sigma}} \right\rangle,$$

where  $K$  is the relativistic nucleon kinetic energy, including its mass. The potential  $V(\bar{\sigma})$  is expressed as in QMC $\pi$ -II, where it adds an additional parameter  $\lambda_3$  to account for the self-coupling of the  $\sigma$  meson. One of the main improvements in this new version is that we employ the full expansion for the  $\sigma$  field solution,  $g_\sigma \bar{\sigma}$ , instead of using a Padé approximant. This solution can be explicitly written in terms of the particle density  $\rho$  and the kinetic energy density  $\tau$  as

$$g_\sigma \bar{\sigma} = v(\rho, \tau, \nabla^2 \rho, (\vec{\nabla} \rho)^2) = v_0(\rho) + v_1(\rho)\tau + v_2(\rho)\nabla^2 \rho + v_3(\rho)(\vec{\nabla} \rho)^2, \quad (1)$$

where

$$\begin{aligned} v_0 &= \frac{-(1 + G_\sigma d \rho) + \sqrt{(1 + G_\sigma d \rho)^2 + 2G_\sigma^2 \lambda_3 \rho}}{\lambda_3 G_\sigma}, \\ v_1 &= \frac{-v'_0(\rho)}{2M_{\text{QMC}}^2(v_0(\rho))}, \\ v_2 &= \frac{1}{\lambda_3 G_\sigma v_0(\rho) + (1 + dG_\sigma \rho)} \frac{v'_0(\rho)}{m_\sigma^2} + \frac{v'_0(\rho)}{4M_{\text{QMC}}^2(v_0(\rho))}, \\ v_3 &= \frac{1}{\lambda_3 G_\sigma v_0(\rho) + (1 + dG_\sigma \rho)} \frac{v''_0(\rho)}{m_\sigma^2}. \end{aligned} \quad (2)$$

As before, the coupling parameter is defined as  $G_\sigma = g_\sigma^2/m_\sigma^2$  where the  $\sigma$  meson mass  $m_\sigma$  is taken as a free parameter in the model. Using the expressions for  $H_{\text{mean}}^\sigma$  and  $H_{\text{fluc}}^\sigma$  in Ref. [9] and upon simplification using the new expressions for  $g_\sigma \bar{\sigma}$  and  $M_{\text{QMC}}(\bar{\sigma})$ , we then solve for the expectation value of the  $\sigma$  Hamiltonian.

The new  $\sigma$  contribution to the total QMC Hamiltonian is now expressed as

$$\begin{aligned}
\langle H_{\text{QMC}\pi\text{-III}}^\sigma \rangle &= h_0(\rho) + h_4(\rho)(J_p^2 + J_n^2) + \sum_{f=p,n} h_1^f(\rho_p, \rho_n)\tau_f \\
&\quad + \sum_{f=p,n} h_2^f(\rho_p, \rho_n)\nabla^2\rho_f + \sum_{f,g=p,n} h_3^{fg}(\rho_p, \rho_n)\vec{\nabla}\rho_f \cdot \vec{\nabla}\rho_g,
\end{aligned}$$

where the coefficients are defined as

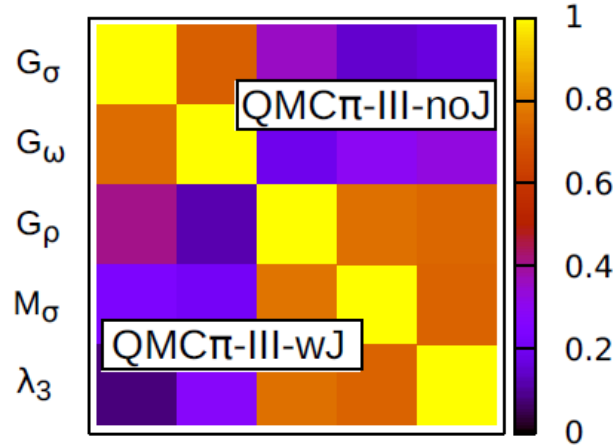
$$\begin{aligned}
h_0(\rho) &= M_{\text{QMC}}(v_0)\rho + \frac{1}{2G_\sigma}v_0^2 + \frac{\lambda_3}{3!}v_0^3 + \frac{1}{4}G_\sigma(1-dv_0)^2(\rho_p^2 + \rho_n^2), \\
h_1^f(\rho_p, \rho_n) &= \frac{1}{2M_{\text{QMC}}(v_0)} - \frac{1}{4}\left[\frac{2dv_1G_\sigma(1-dv_0)^2}{1-dv_0}\right](\rho_p^2 + \rho_n^2) - \frac{1}{2}q(\rho)\rho_f, \\
h_2^f(\rho_p, \rho_n) &= -\frac{1}{4M_{\text{QMC}}(v_0)} - \frac{1}{4}\left[\frac{2dv_2G_\sigma(1-dv_0)^2}{1-dv_0}\right](\rho_p^2 + \rho_n^2) + \frac{1}{4}q(\rho)\rho_f, \\
h_3^{fg}(\rho_p, \rho_n) &= \frac{v_0'^2}{2m_\sigma^2G_\sigma} - \frac{1}{4}\left[\frac{2dv_3G_\sigma(1-dv_0)^2}{1-dv_0} + p^2\right](\rho_p^2 + \rho_n^2) + \delta(f, g)\frac{1}{8}p^2, \\
h_4(\rho) &= \frac{1}{4}p^2,
\end{aligned}$$

with  $p(\rho) = \frac{-\sqrt{G_\sigma}(1-dv_0)}{m_\sigma}$  and  $q(\rho) = (1 + \frac{m_\sigma^2}{2M_{\text{QMC}}^2(v_0)})p^2$ .

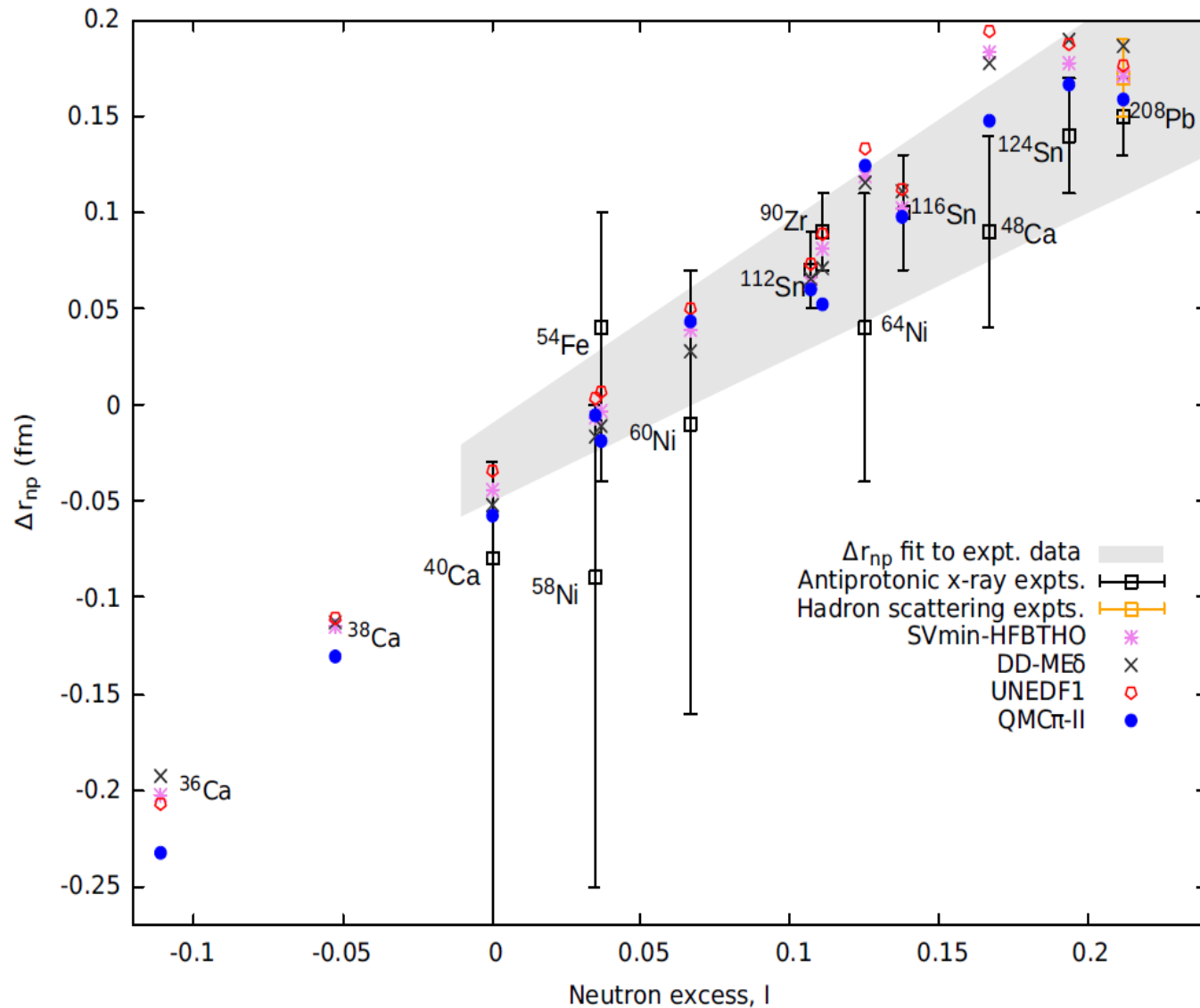
TABLE I. QMC $\pi$ -III parameters and NMPs along with their errors written in parentheses.

Parameter	QMC $\pi$ -III-wJ		QMC $\pi$ -III-noJ		NMP	QMC $\pi$ -III-wJ	QMC $\pi$ -III-noJ
$G_\sigma$ [fm $^{-2}$ ]	9.62	(0.01)	9.66	(0.02)	$\rho_0$ [fm $^{-3}$ ]	0.15	0.15
$G_\omega$ [fm $^{-2}$ ]	5.21	(0.01)	5.28	(0.01)	$E_0$ [MeV]	-15.7	-15.7
$G_\rho$ [fm $^{-2}$ ]	4.71	(0.03)	4.75	(0.03)	$a_{sym}$ [MeV]	29	29
$m_\sigma$ [MeV]	504	(1)	504	(1)	$L_0$ [MeV]	43	43
$\lambda_3$ [fm $^{-1}$ ]	0.05	(0.01)	0.05	(0.01)	$K_0$ [MeV]	233	235

correlation with the other parameters. Meanwhile,  $G_\rho$  is highly correlated with both  $m_\sigma$  and  $\lambda_3$  and just as in QMC $\pi$ -II, the  $\sigma$  meson mass also has high correlation with  $\lambda_3$ .



# Neutron distributions



Kay Martinez *et al.*, Phys Rev C100 (2019) 024333

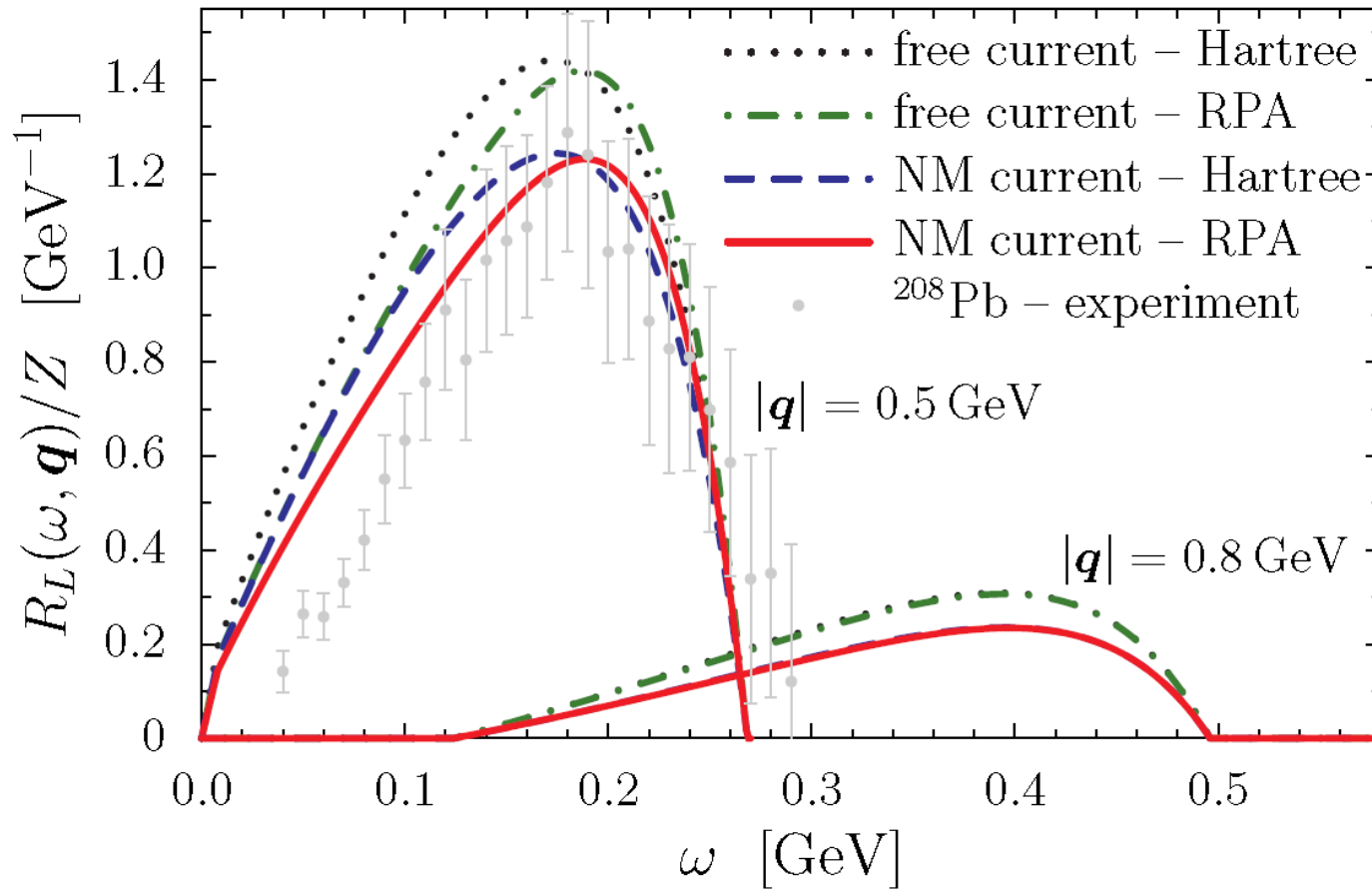
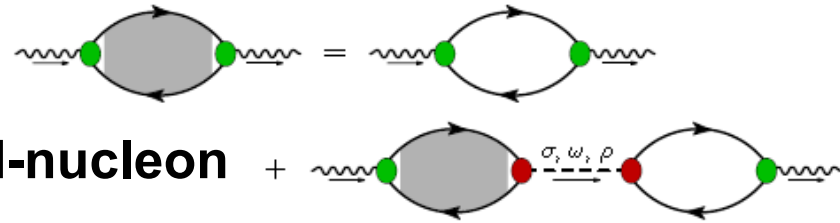


# Modified Electromagnetic Form Factors In-Medium

# Response Function

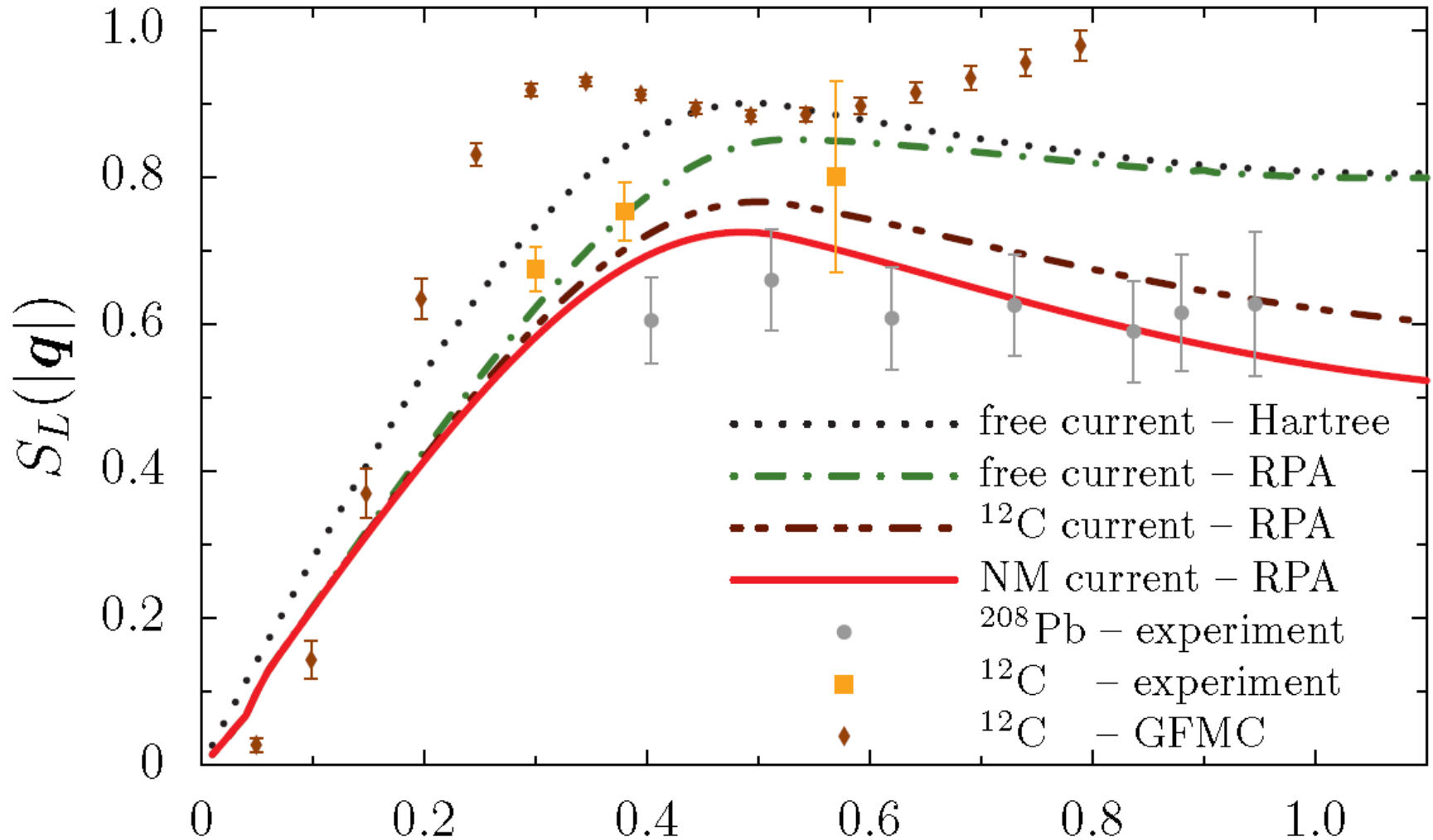
$$\frac{d^2\sigma}{d\Omega d\omega} = \sigma_{\text{Mott}} \left[ \frac{q^4}{|\mathbf{q}|^4} R_L(\omega, |\mathbf{q}|) + \left( \frac{q^2}{2|\mathbf{q}|^2} + \tan^2 \frac{\theta}{2} \right) R_T(\omega, |\mathbf{q}|) \right]$$

RPA correlations repulsive  
 Significant reduction in Response  
 Function from the modification of bound-nucleon



Cloët, Bentz & Thomas, PRL 116 (2016) 032701

# Comparison with Unmodified Nucleon & Data



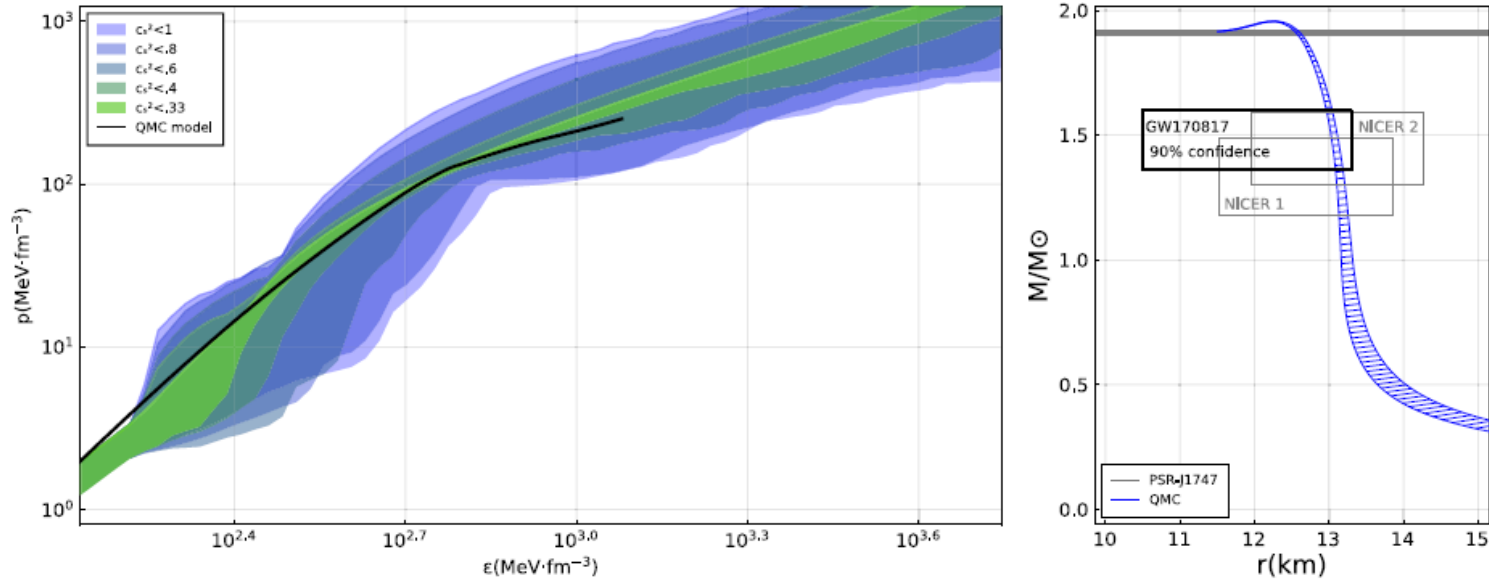
$$S_L(|\mathbf{q}|) = \int_{\omega+}^{|\mathbf{q}|} d\omega \frac{R_L(\omega, |\mathbf{q}|)}{Z G_{Ep}^2(Q^2) + N G_{En}^2(Q^2)} |\mathbf{q}| \text{ [GeV]}$$

**Data: Morgenstern & Meziani**

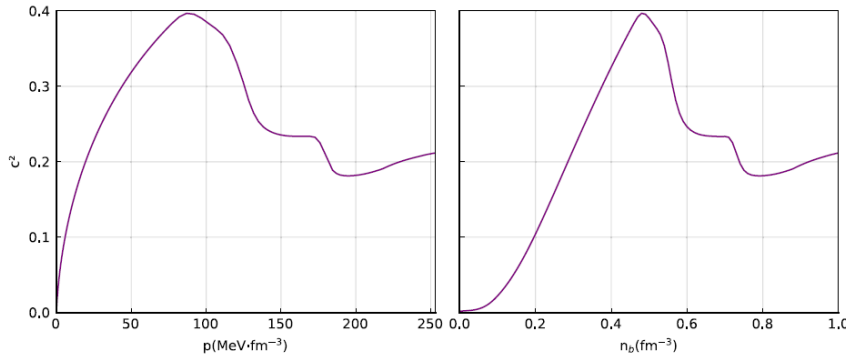
**Calculations: Cloët, Bentz & Thomas (PRL 116 (2016) 032701)**

# On the sound speed in hyperonic stars

T.F. Motta <sup>a,\*</sup>, P.A.M. Guichon <sup>b</sup>, A.W. Thomas <sup>a</sup>



**Follow up on Annala et al., Nature Physics (2020) model independent EoS based on speed of sound interpolation between low and high density - claim low value implies quark matter**





# Spectroscopy

- how do excited states emerge from QCD ?
- what are the fundamental degrees of freedom ?
- Lattice QCD provides extremely valuable information

# The $\Lambda(1405)$

- We have unambiguous evidence that it is a  $K\bar{N}$  bound state!  
50 years after speculation by Dalitz *et al.*
- To be fair Dalitz had no quark model then so there was not much else it could be at that time.
- Rather than the Lüscher method we apply **Hamiltonian Effective Field Theory**
  - shown to be equivalent for phase shifts\*
  - **BUT also provides information on eigenstates**
- Carry out a Hamiltonian analysis of lattice data
- Examine the **strange magnetic form factor** of  $\Lambda(1405)$

\* Wu *et al.*, Phys. Rev. C 90 (2014) 5, 055206

# First calculation after QCD was invented incorporating chiral symmetry

PHYSICAL REVIEW D

VOLUME 31, NUMBER 5

1 MARCH 1985

## *S*-wave meson-nucleon scattering in an SU(3) cloudy bag model

E. A. Veit\* and B. K. Jennings

*TRIUMF, 4004 Wesbrook Mall, Vancouver, British Columbia, Canada V6T 2A3*

A. W. Thomas

*Physics Department, University of Adelaide, Adelaide, South Australia 5001*

R. C. Barrett

*Physics Department, University of Surrey, Guildford GU2 5XH, United Kingdom*

(Received 8 June 1984)

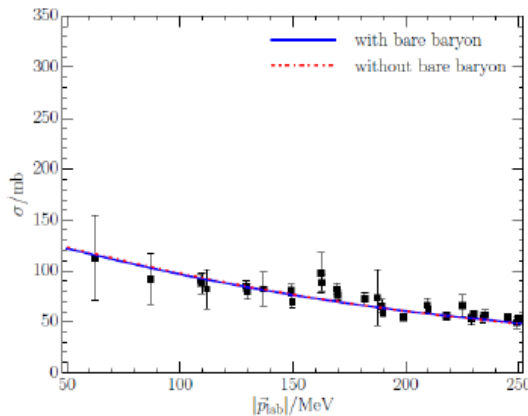
The cloudy bag model (CBM) is extended to incorporate chiral  $SU(3) \times SU(3)$  symmetry, in order to describe *S*-wave  $KN$  and  $\bar{K}N$  scattering. In spite of the large mass of the kaon, the model yields reasonable results once the physical masses of the mesons are used. We use that version of the CBM in which the mesons couple to the quarks with an axial-vector coupling throughout the bag volume. This version also has a meson-quark contact interaction with the same spin-flavor structure as the exchange of the octet of vector mesons. The present model strongly supports the contention that the  $\Lambda^*(1405)$  is a  $\bar{K}N$  bound state.

But now we can use QCD itself

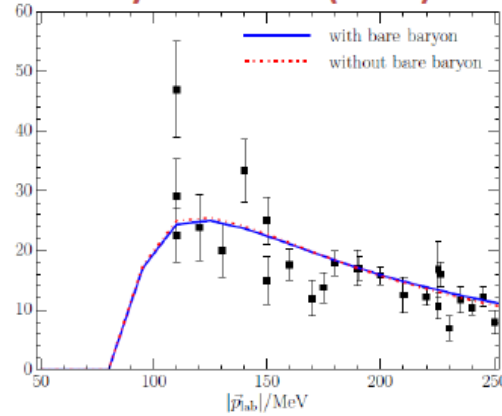


# Hamiltonian fit to existing data

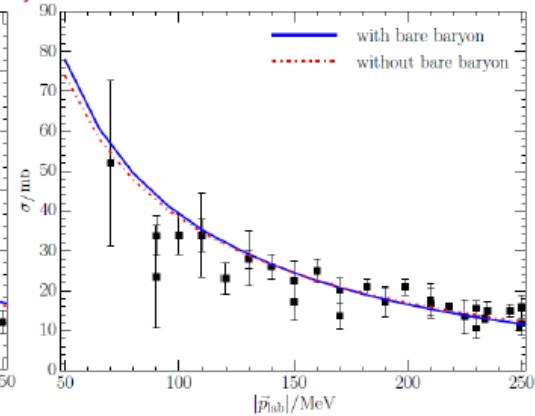
Zhan-wei Liu etc. Phys.Rev. D95 (2017) no.1, 014506



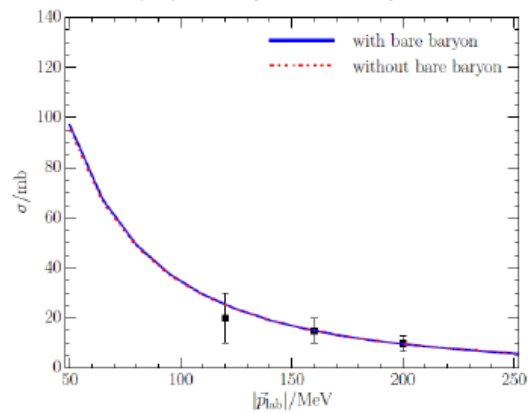
(a)  $K^- p \rightarrow K^- p$



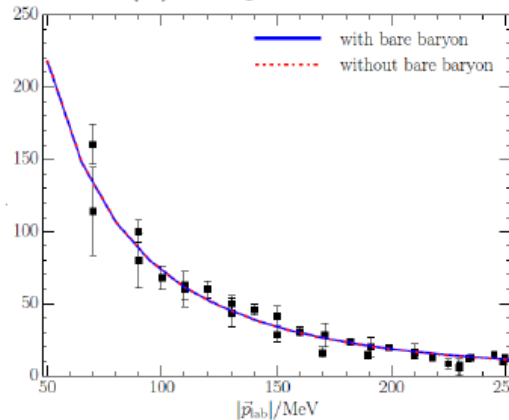
(b)  $K^- p \rightarrow \bar{K}^0 n$



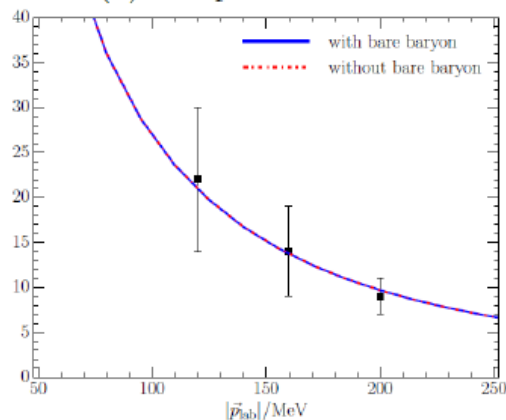
(c)  $K^- p \rightarrow \pi^- \Sigma^+$



(d)  $K^- p \rightarrow \pi^0 \Sigma^0$



(e)  $K^- p \rightarrow \pi^+ \Sigma^-$



(f)  $K^- p \rightarrow \pi^0 \Lambda$

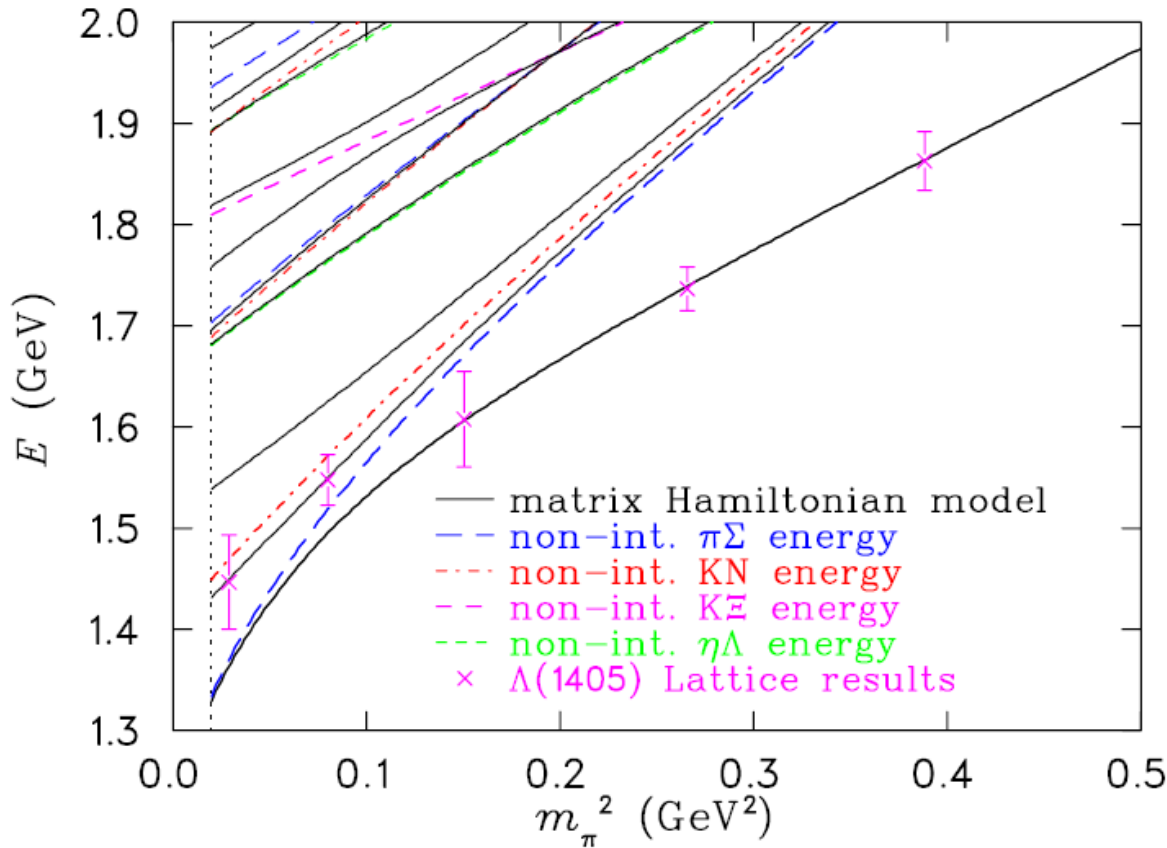
Include  $\pi\Sigma$ ,  $\bar{K}N$ ,  $\eta\Lambda$  and  $K\Xi$  channels

Similar work by Valencia, Bonn, JLab and other groups

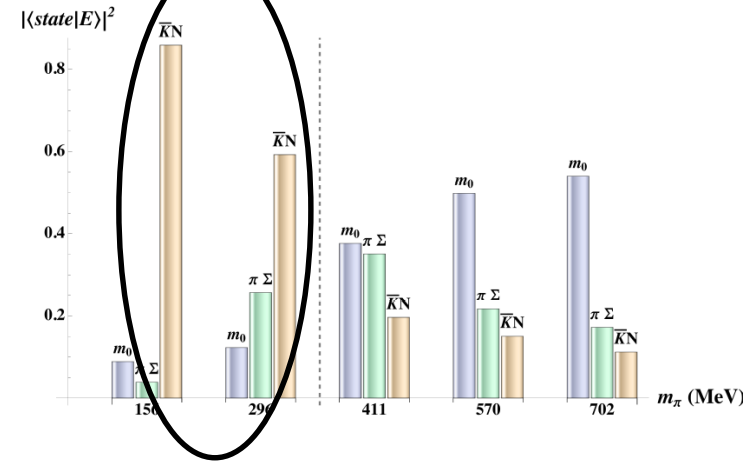
Find the same two-pole structure as other analyses

# Low lying negative parity state : $\Lambda(1405)$

Clear evidence that it is a  $\bar{K}N$  bound state



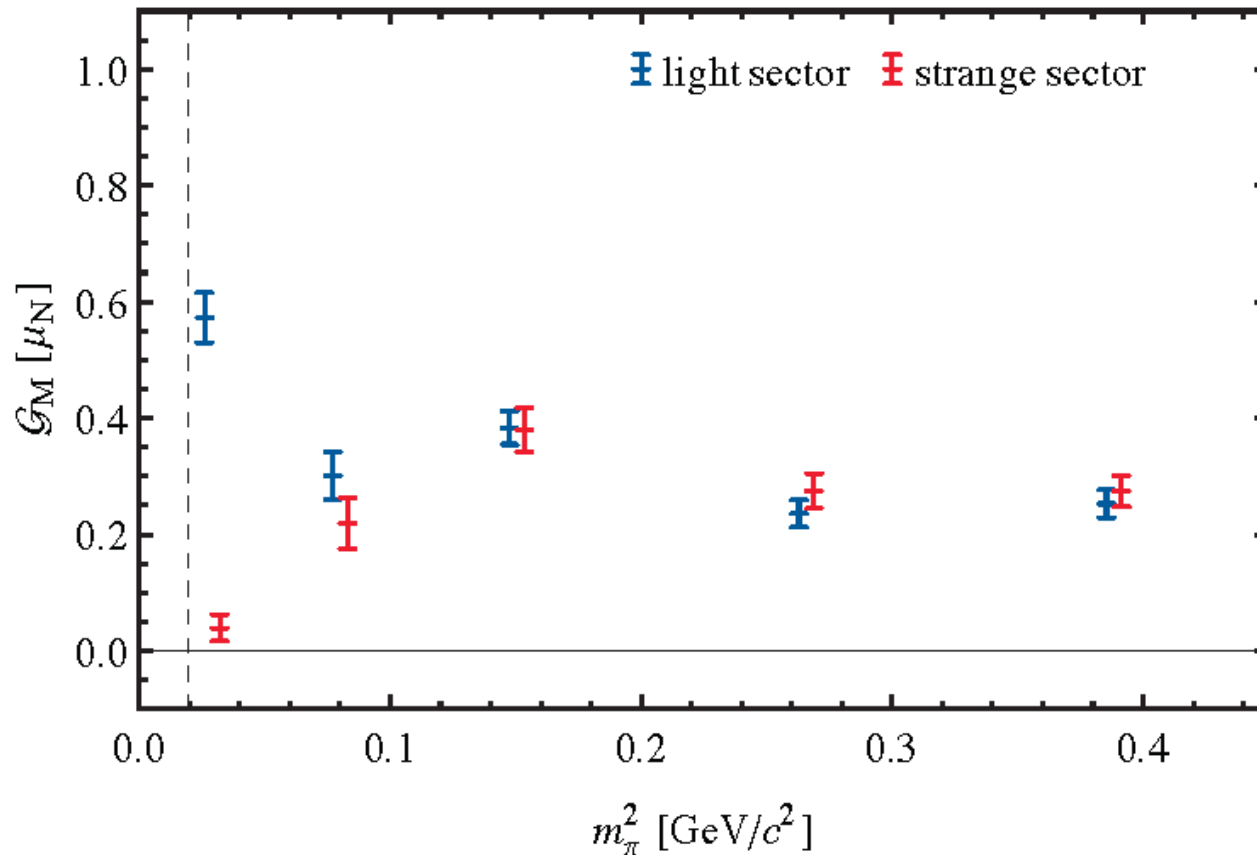
Hamiltonian approach allows one to examine the eigenstates:



Hall, Leinweber, Menadue, Young, AWT  
 – Phys. Rev. Lett. 114 (2015) 13

# Lattice Magnetic Form Factor Calculations

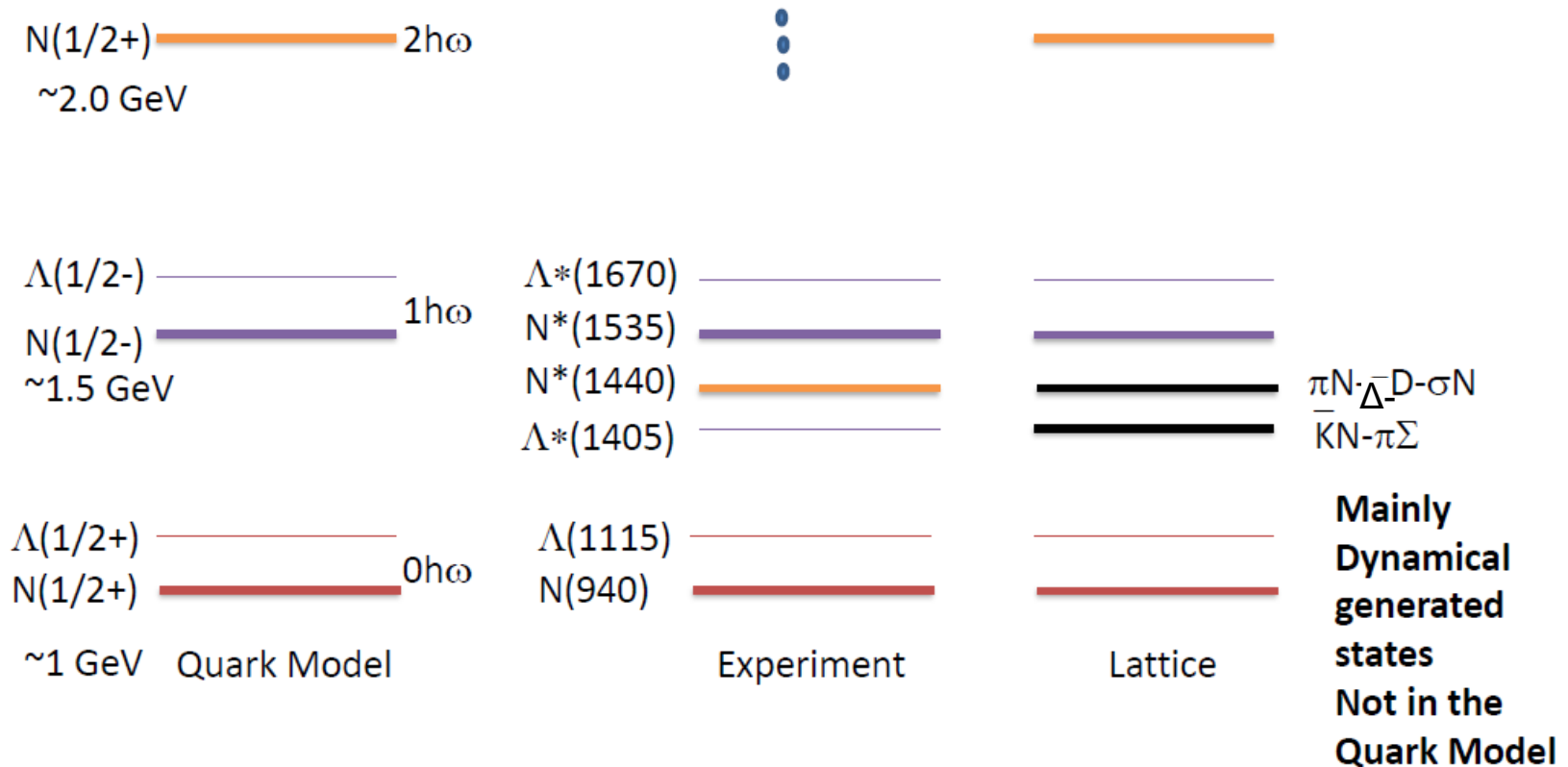
- Calculation of the individual quark contributions to the magnetic form factor confirms that it is a  $K\bar{u}N$  bound state



Only an  $L=0$   $K\bar{u}N$  state gives vanishing strange moment

**Note that Lattice QCD allows  
us to study hadron structure IN QCD as a  
function of quark mass – a powerful tool\***

# Once the nature of key states becomes clear the quark model makes sense



# Summary

- **New techniques applied to lattice QCD provide hitherto unimagined insights into hadron structure**
- **Neither the  $\Lambda(1405)$  nor the Roper are predominantly three-quark states**
- **The quark model has new life with ordering of major shells as expected**
- **These insights may well resolve “missing state” problem**